Molecular Therapy
Nucleic Acids
Original Article

Cell-targeted gene modification by delivery of CRISPR-Cas9 ribonucleoprotein complexes in pseudotyped lentivirus-derived nanoparticles

Ian Helstrup Nielsen,[1] Anne Bruun Rovsing,[1] Jacob Hørlück Janns,[1] Emil Aagaard Thomsen,[1] Albert Ruzo,[2] Andreas Bøggild,[3] Frederikke Nedergaard,[1] Charlotte Thornild Møller,[1] Thomas Boesen,[3] Søren Egedal Degn,[1] Jagesh V. Shah,[2] and Jacob Giehm Mikkelsen[1]

[1]Department of Biomedicine, Aarhus University, Høegh-Guldbergs Gade 10, 8000 Aarhus C, Denmark; [2]Sana Biotechnology, Inc, Cambridge, MA 02139, USA; [3]Interdisciplinary Nanoscience Center (iNANO), Aarhus University, 8000 Aarhus C, Denmark

To fully utilize the potential of CRISPR-Cas9-mediated genome editing, time-restricted and targeted delivery is crucial. By modulating the pseudotype of engineered lentivirus-derived nanoparticles (LVNPs), we demonstrate efficient cell-targeted delivery of Cas9/single guide RNA (sgRNA) ribonucleoprotein (RNP) complexes, supporting gene modification in a defined subset of cells in mixed cell populations. LVNPs pseudotyped with severe acute respiratory syndrome coronavirus 2 (SARS-CoV-2) spike protein resulted in angiotensin-converting enzyme 2 (ACE2)-dependent insertion or deletion (indel) formation in an $ACE2^{+}/ACE2^{-}$ population of cells, whereas Nipah virus glycoprotein pseudotyping resulted in Ephrin-B2/B3-specific gene knockout. Additionally, LVNPs pseudotyped with Edmonston strain measles virus glycoproteins (MV-H/F) delivered Cas9/sgRNA RNPs to $CD46^{+}$ cells with and without additional expression of SLAM (signaling lymphocytic activation molecule; CD150). However, an engineered SLAM-specific measles virus pseudotype (measles virus-hemagglutinin/fusion [MV-H/F]-SLAM) efficiently targeted LVNPs to $SLAM^{+}$ cells. Lentiviral vectors (LVs) pseudotyped with MV-H/F-SLAM efficiently transduced >80% of interleukin (IL)-4/IL-21-stimulated primary B cells cultured on CD40 ligand (CD40L)-expressing feeder cells. Notably, LVNPs pseudotyped with MV-H/F and MV-H/F-SLAM reached indel rates of >80% and >60% in stimulated primary B cells, respectively. Collectively, our findings demonstrate the modularity of LVNP-directed delivery of ready-to-function Cas9/sgRNA complexes. Using a panel of different pseudotypes, we provide evidence that LVNPs can be engineered to induce effective indel formation in a subpopulation of cells defined by the expression of surface receptors.

INTRODUCTION

Endonuclease-based genome editing is a fast-moving and heavily investigated approach for targeted gene correction and potential therapeutic use. With the discovery of the clustered regularly interspaced short palindromic repeats (CRISPR) system,[1–4] genome editing has become widely accessible, and several ongoing clinical trials bear witness to high expectations from the industry. With a rapidly expanding genome editing toolbox, including CRISPR-Cas9 and numerous derived technologies like base and prime editing, as well as CRISPR gene inhibition and activation systems, innovation of approaches for the delivery of genome-modifying tools has become pivotal. As natural carriers of genetic material, viruses have, over the years, been adapted for receptor-targeted delivery of genetic information, providing gene delivery technologies for gene therapy.[5,6] Due to their capacity to transduce non-dividing cells, lentiviral vectors (LVs) derived from human immunodeficiency virus type 1 (HIV-1) have been widely used to deliver and integrate therapeutically relevant genes both *ex vivo* and *in vivo*.[7,8] To further exploit the applications of viruses to ferry cargo, we and others have developed protein fusion strategies to incorporate and deliver therapeutic proteins in enveloped virus-derived particles.[9–20] Retroviruses, like HIV-1, are assembled at the plasma membrane as aggregates of Gag and GagPol polypeptides carrying structural and enzymatic proteins. This process ensures that all viral proteins are included in a certain ratio in particles budding from the membrane. To incorporate a foreign protein of interest in viral particles, the protein can be fused to the polypeptides, most often to the N or C terminus of Gag. Upon maturation of the virus particle, driven by the cleavage of Gag and GagPol into smaller entities by the viral protease, the fused protein is released from the polypeptides and may exert its function in recipient cells. Recently, we adapted lentivirus-derived nanoparticles (LVNPs) for transient delivery of Cas9/single guide RNA (sgRNA) ribonucleoprotein (RNP) complexes, supporting potent DNA cleavage and insertion or deletion (indel) formation in recipient cells both *ex vivo* and *in vivo*, including in the mouse retina.[21]

The tropism of enveloped lentivirus-based vectors and protein delivery vehicles is determined by glycoproteins embedded in the lipid

Received 22 May 2024; accepted 29 August 2024;
https://doi.org/10.1016/j.omtn.2024.102318.

Correspondence: Jacob Giehm Mikkelsen, Department of Biomedicine, Aarhus University, Høegh-Guldbergs Gade 10, 8000 Aarhus C, Denmark.
E-mail: giehm@biomed.au.dk

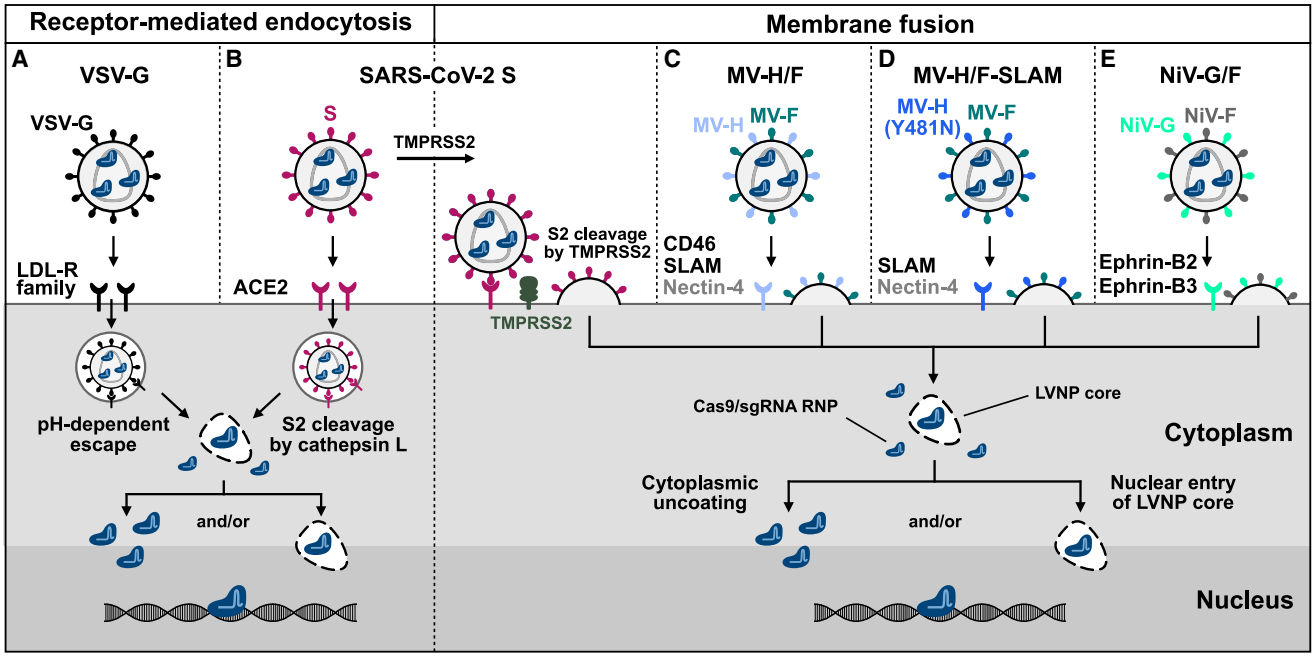

Figure 1. Overview of the presented pseudotypes and their natural target receptors and entry pathways

(A) Vesicular stomatitis virus glycoprotein (VSV-G) recognizes and binds members of the LDL receptor (LDL-R) family. Entry happens through receptor-mediated endocytosis, and the LVNP cargo is released after endosomal escape. (B) SARS-CoV-2 S binds to ACE2 receptors. Without TMPRSS2 cleavage, entry is mediated by receptor-mediated endocytosis, whereas with TMPRSS2 cleavage, fusion occurs at the cell membrane. (C) Measles virus hemagglutinin (MV-H) recognizes CD46, SLAM (CD150), and Nectin-4. Entry occurs by fusion at the cell membrane initiated by conformational changes in the fusion proteins (MV-F), and the cargo is thereby released to the cytoplasm. (D) The Y481N mutation in the MV-H proteins has blinded the affinity toward CD46, and it will therefore only recognize SLAM (and Nectin-4). (E) Nipah virus attachment protein (NiV-G) binds Ephrin-B2 and/or Ephrin-B3. Entry happens through fusion at the cell membrane.

bilayer membrane surrounding the particle core, which mediate binding to receptors leading to entry into the target cell.[22] This configuration of glycoproteins defines the pseudotype. Pseudotyping refers to the process of generating viruses or virus-derived vehicles carrying envelope (Env) proteins derived from other viruses or proteins engineered to bind to a certain receptor. Naturally occurring glycoproteins are frequently used to achieve cell-targeted lentiviral gene transfer.[23] The range of tropisms of LVs has been further expanded by coating viral particles carrying vector RNA with engineered surface proteins, like glycoprotein-based single-chain antibody fusogens.[24,25] The vesicular stomatitis virus glycoprotein (VSV-G) has been adapted as a standard pseudotype for LVs.[26] VSV-G targets receptors of the low-density lipoprotein (LDL) receptor family, which are expressed in most tissues and cells, and VSV-G therefore offers a wide tropism supporting many different delivery purposes.[27] VSV-G-directed cell entry occurs through receptor-mediated endocytosis, and subsequent pH-induced endosomal escape results in the release of the viral cargo to the cytoplasm (Figure 1A).[28] Pseudotyping of viruses with the severe acute respiratory syndrome coronavirus 2 (SARS-CoV-2) spike (S) protein has been utilized to analyze immunization and the capacity of newly emerged S variants to support infectivity.[29–33] The S protein binds angiotensin-converting enzyme 2 (ACE2), mediating entry through receptor-mediated endocytosis. The viral cargo is released into the cytoplasm after cleavage of the S2 subunit by cathepsin L in the endosome. However, an alternative entry pathway, involving membrane fusion based on the cleavage of S2 by TMPRSS2 at the cell membrane after ACE2 binding, has been reported (Figure 1B).[34,35] Another pseudotype is based on incorporation of the measles virus hemagglutinin (MV-H) and fusion (MV-F) proteins in the membrane surrounding the lentiviral particle.[36–38] MV effectively targets immune cells, including T and B cells, due to the capacity of the MV-H protein to interact with signaling lymphocytic activation molecule (SLAM; also referred to as CD150) present on the surface of immune cells. The target receptors of naturally occurring MV include SLAM and the epithelial nectin-4 protein.[39–41] However, MV-H from the Edmonston vaccine strain has acquired an additional tropism for the membrane cofactor protein (MCP; CD46) found on nucleated cells.[42] After binding to a target receptor, the MV-H protein triggers conformational changes in the MV-F protein, which subsequently induces fusion at the host cell membrane (Figure 1C). The affinity for CD46 can be eliminated by introducing a Y481N mutation in the Edmonston MV-H protein, thereby restoring the natural tropism (Figure 1D).[38] Like MV, Nipah virus (NiV) belongs to the family *Paramyxoviridae*, and the NiV attachment (NiV-G) and fusion (NiV-F) proteins have a high resemblance to the corresponding MV proteins. Ephrin-B2 and Ephrin-B3 serve as receptors for NiV-G protein, ultimately leading to fusion between the viral Env and the cell membrane (Figure 1E).[43,44] It has been reported that both NiV and

MV glycoprotein-mediated entry can occur through macropinocytosis as well.[38,45] Gene delivery to cells expressing Ephrin-B2 has been achieved with NiV-pseudotyped LVs.[46,47] Furthermore, MV- and NiV-derived fusogens have been engineered for targeted lentiviral gene delivery using alternative cell-specific receptors.[25,48]

B cells and thereof derived plasma cells are important mediators of the adaptive humoral immune response.[49] B cells interact with primed T cells by presenting foreign antigens on major histocompatibility complex (MHC) class II. Furthermore, memory B cells and long-lived plasma cells are important for sustaining long-term immunity.[50] The ability of B lineage cells to secrete large amounts of antibodies and their involvement in autoimmune diseases make these cells important targets for gene therapies, including genome editing. High-efficacy targeted DNA modification has been reported in primary B cells after activation and *ex vivo* electroporation with RNP complexes consisting of recombinant Cas9 and synthetic sgRNAs. Combined with treatment with adeno-associated virus (AAV) carrying a DNA repair donor or transfection with single-stranded DNA oligonucleotides (ssODNs), targeted DNA cleavage supports homology-directed repair (HDR) leading to gene editing.[51–56]

LVNPs offer a novel approach for cell-targeted delivery of CRISPR-Cas9 RNPs to primary cells using different pseudotypes. Evidence is needed, however, to demonstrate both the cell specificity and gene editing efficacy of pseudotyped LVNPs loaded with Cas9/sgRNA in mixed cell populations, including primary cells. Here, we report high levels of cell-specific DNA modification in mixed cell populations using SARS-CoV-2 S protein, as well as NiV- and MV-derived glycoproteins for pseudotyping of LVNPs loaded with CRISPR-Cas9 RNPs. Furthermore, we demonstrate indel rates reaching >80% in human primary B cells treated with MV-H/-F-pseudotyped LVNPs. Our findings highlight the utility of engineered LVNPs carrying different pseudotypes for receptor-specific protein delivery and establish pseudotyped LVNPs as delivery vehicles for cell-targeted RNP delivery, leading to gene modification in different cell types, including primary B cells. Such findings may have relevance for future *in vivo* use.

RESULTS

Targeted DNA modification in cells treated with VSV-G-pseudotyped Cas9/sgRNA-loaded LVNPs

To investigate the cellular delivery of Cas9/sgRNA RNPs using LVNPs, we first produced three separate VSV-G-pseudotyped LVNPs carrying sgRNAs targeting the *AFF1* gene, the *B2M* gene, and the *HEK3* locus. Transfected plasmids and the ratio used for production of VSV-G-pseudotyped LVNPs are illustrated in Figure 2A. In HEK293T cells, VSV-G-pseudotyped LVNPs induced targeted DNA modification, resulting in indel rates >80% in the *AFF1* and *HEK3* loci (Figure 2B) and similar knockout (KO) scores in *B2M* measured by flow cytometric detection of β-2 microglobulin (Figure 2C). Relative to the *HEK3* and *B2M* targets, for which all LVNP dosages induced robust indel formation, efficient cleavage in *AFF1* required higher dosages of LVNPs. LVNP treatment of SupT1 cells illustrated a notable difference between cell types. In these cells, VSV-G-pseudotyped LVNPs induced around 60% indel formation (depending on dose) in the *HEK3* locus, whereas the *AFF1* locus was unaffected by exposure to LVNPs (Figure 2D). We have reproducibly seen that this particular *AFF1* sgRNA does not facilitate indel formation in T cells, most likely due to the reduced accessibility of this target in T cells. *B2M*, in contrast, was effectively targeted in SupT1, resulting in KO scores of 60% using a low dose of LVNPs corresponding to 15 ng p24 (Figure 2E).

Cell-targeted RNP delivery to ACE2-expressing cells by LVNPs pseudotyped with SARS-CoV-2 S protein

To study the capacity of LVNPs to deliver Cas9/sgRNA RNPs to a defined subset of cells within a population of cells, we wanted to explore the use of SARS-CoV-2 S protein for pseudotyping of LVs and LVNPs produced using the ratios of transfected plasmids shown in Figures 3A and 3B, respectively. To optimize the transfer of cargo, we used a truncated version of the S protein (SΔ19; lacking 19 amino acids in the cytoplasmic tail), which has previously been found to increase the incorporation of the glycoprotein in the viral membrane.[31,57] Initial titer experiments demonstrated that unconcentrated LVs pseudotyped with SARS-CoV-2 S protein (based on SARS-CoV-2 S or the S(N501Y) variant derived from SARS-CoV-2 B.1.1.7) did not transduce HEK293T cells (Figure 3C). However, in HEK293T cells engineered to express the ACE2 receptor (HEK293T/ACE2$^+$) (Figure S1A), titers of 5×10^4 IU/mL were obtained with both S protein variants. Still, titers were about 100-fold lower than for VSV-G-pseudotyped LVs (Figure 3D).

To pseudotype LVNPs for editing in ACE2$^+$ cells, we used the S(N501Y) pseudotype, which has been reported to increase the affinity for cellular receptors and thereby enhance infectivity.[58] Initially, we produced LVNPs carrying both Cas9/sgRNA RNPs (targeting *B2M*) and vector RNA encoding eGFP and concentrated these by ultracentrifugation. This resulted in higher titers for both VSV-G and S(N501Y)-pseudotyped LVNPs in HEK293T/ACE2$^+$ cells but, again, showed a markedly higher titer for VSV-G-pseudotyped LVNPs (Figure 3E). Using serially diluted LVNPs (based on ng p24), we then measured both *EGFP* gene transfer and *B2M* KO rates for increasing LVNP dosages and found correlating effects on *EGFP* gene and Cas9/sgRNA RNP transfer (Figures 3F–3H). Hence, for the lower dosages, only VSV-G-pseudotyped LVNPs were able to support gene transfer and RNP delivery leading to *B2M* KO. Notably, with the highest dose tested (50 ng p24), S(N501Y)-pseudotyped LVNPs reached near-maximum activity with >80% cells transduced (Figure 3F) and a *B2M* KO rate of 80% (Figures 3H and S2A). We performed a similar experiment for LVNPs carrying sgRNAs targeting the *AFF1* gene and observed again that the higher dosages of S(N501Y)-pseudotyped LVNPs were required to support indel formation (Figure 3I). Based on the measurements of transductional titers (IU/mL) determined in HEK293T/ACE2$^+$ cells, we estimated that a multiplicity of infection (MOI) of ∼60 (IU/cell; 2.5×10^6 IU added to 4×10^4 cells) resulted in 60% *B2M* KO using VSV-G-pseudotyped LVNPs. In contrast, for S(N501Y)-pseudotyped LVNPs, an MOI of ∼1

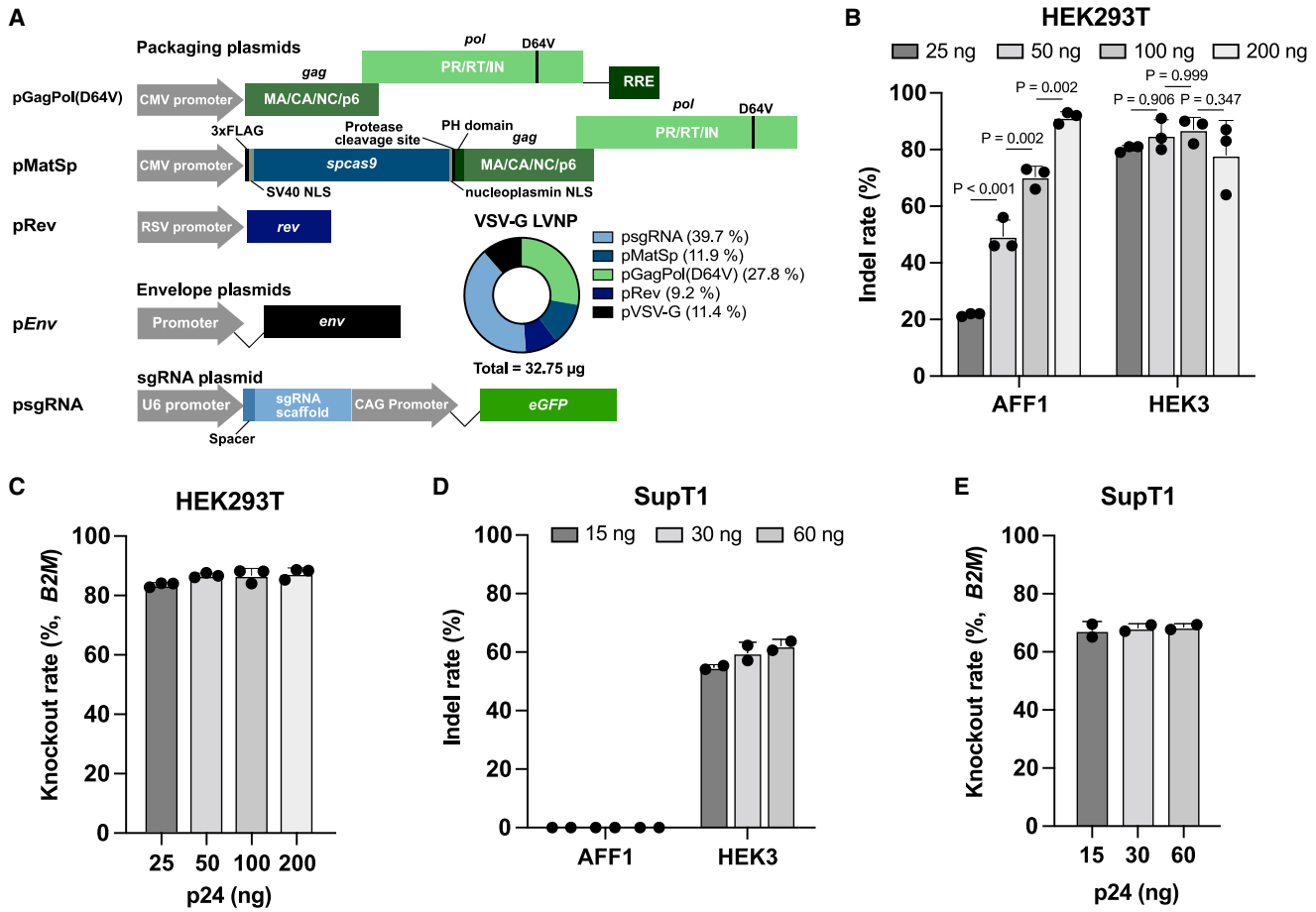

Figure 2. Targeted DNA modification in cells treated with VSV-G-pseudotyped CRISPR-Cas9/sgRNA-loaded LVNPs

(A) Plasmids used for production of LVNPs. Plasmids are co-transfected into HEK293T producer cells using the calcium phosphate method. Donut diagram shows the amounts of the different plasmids used in a transfection for the production of VSV-G-pseudotyped LVNPs. (B) 8×10^4 HEK293T cells were treated with increasing dosages of VSV-G-pseudotyped LVNPs targeting *AFF1* or *HEK3*. Indel rates were determined 3 days after transduction (n = 3 technical replicates). (C) 8×10^4 HEK293T cells were treated with increasing dosages of VSV-G-pseudotyped LVNPs targeting *B2M*. KO rates were determined by flow cytometry after 7 days using an anti-B2M-PE antibody (n = 3 technical replicates). (D) Indel rates determined 3 days after treating 1×10^5 SupT1 cells with increasing dosages of VSV-G-pseudotyped LVNPs targeting *AFF1* or *HEK3* (n = 2 technical replicates). (E) 1×10^5 SupT1 cells were treated with increasing dosages of VSV-G-pseudotyped LVNPs targeting *B2M*. KO rates were determined by flow cytometry after 7 days using an anti-B2M-PE antibody (n = 2 technical replicates). Data are presented as mean (SD). Indel rates were determined by ICE analysis.

supported 80% KO in HEK293T/ACE2$^+$ cells. Notably, as these estimations were based on relating KO rates with the vector-transferring capacity (the latter based on determining the number of particles supporting *EGFP* transfer and expression), they did not include Cas9/sgRNA-loaded particles devoid of vector RNA or particles that did not support functional gene transfer leading to expression. Hence, as the vector transfer capacity of S(N501Y)-pseudotyped lentiviral particles, most likely due to reduced cellular entry of particles carrying this particular pseudotype in HEK293/ACE2+ cells, the resulting MOI supporting KO was low based on this calculation. Therefore, we suspect that the actual number of LVNPs per recipient cell was likely to be higher. Additionally, we measured the viability of the cells upon LVNP exposure and, overall, did not observe any impact of the LVNPs relative to untreated cells (Figures S2B and S2C). Also, we did not see any clear differences between the two pseudotypes.

Next, a mixed population of cells consisting of ACE2$^+$/eGFP$^-$ (Figure S1A) and ACE2$^-$/eGFP$^+$ (Figure S1B) HEK293T cells (seeded in a 1:1 ratio) were treated with LVNPs pseudotyped with either VSV-G or SARS-CoV-2 S(N501Y) (Figure 3I). To challenge the specificity of the S(N501Y) pseudotype for the ACE2 receptor, we used dosages corresponding to 500 ng p24 in this experiment, ensuring potent indel formation in susceptible cells. Seven days after treatment, the cells were sorted based on their eGFP and ACE2 expression. Subsequent indel analyses of the sorted cell populations showed indel rates of 100% in the *AFF1* gene of ACE2$^+$ cells exposed to S(N501Y)-pseudotyped LVNPs and no indel formation in ACE2$^-$ cells (Figure 3J). As expected, VSV-G-pseudotyped LVNPs did not discriminate between ACE2$^+$ and ACE2$^-$ cells and efficiently induced indel formation in both cell types (Figure 3J). These data demonstrate the capacity of LVNPs to deliver

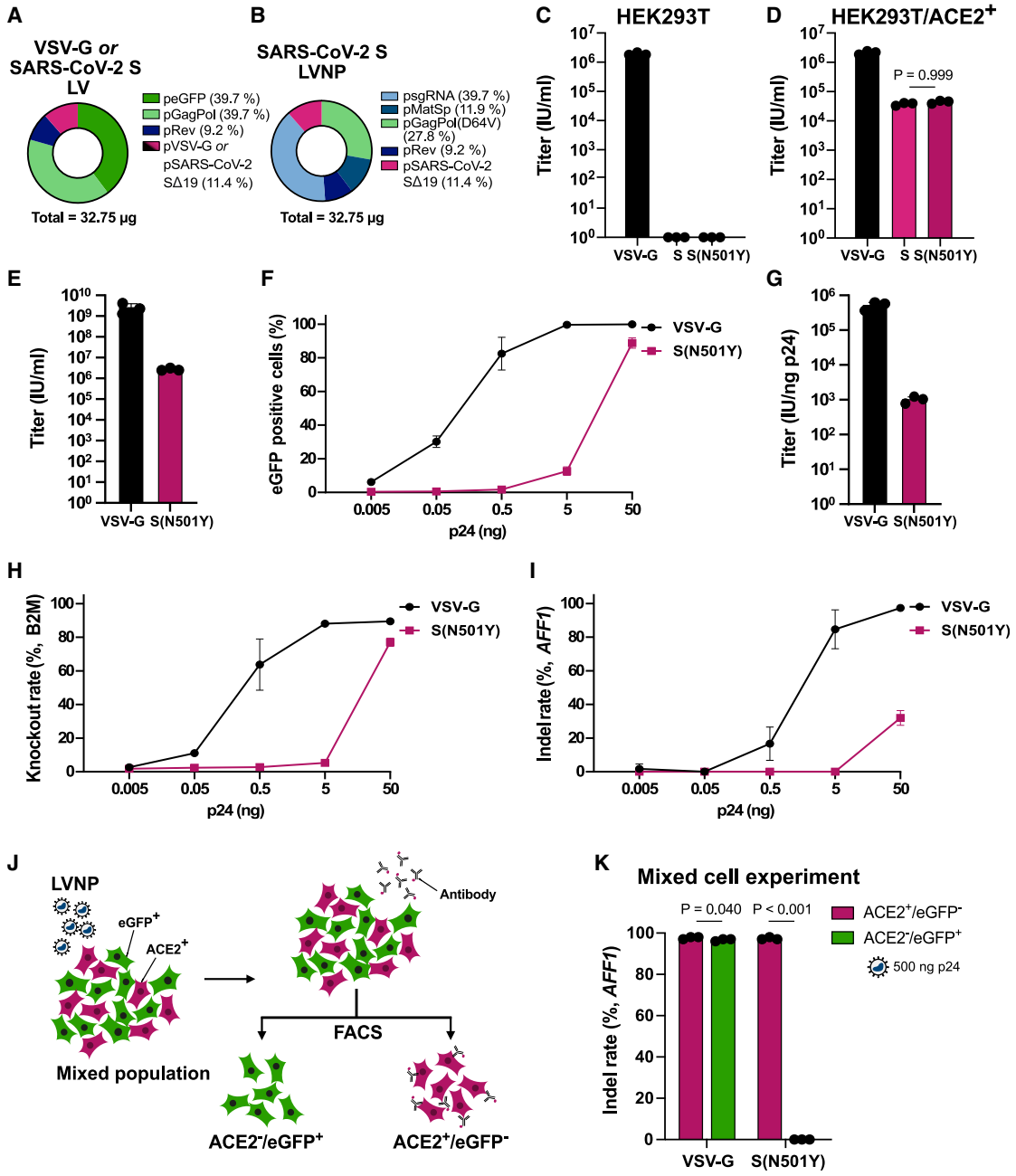

Figure 3. SARS-CoV-2 S-pseudotyped LVNPs specifically deliver RNPs to cells expressing ACE2

(A) Plasmid ratios used for production of VSV-G-pseudotyped or SARS-CoV-2 S- and S(N501Y)-pseudotyped LVs. (B) Plasmid ratios used for production of S- and S(N501Y)-pseudotyped LVNPs. (C) Transductional titers determined by treating 8×10^4 HEK293T cells with serial dilutions of unconcentrated LVs ($n = 3$ biological replicates). (D) HEK293T/ACE2$^+$ cells were treated with serial dilutions of unconcentrated LVs ($n = 3$ biological replicates). Three days after transduction, eGFP expression was determined by flow cytometry, allowing the shown titers to be calculated. (E) 4×10^4 HEK293T/ACE2$^+$ cells were treated with serial dilutions of ultracentrifuged LVNPs carrying an *EGFP* transfer vector and *B2M*-targeting RNPs. The shown titer (IU/mL) was calculated based on the number of eGFP-positive cells determined by flow cytometry 3 days after transduction ($n = 3$ biological replicates). (F) Dose-response curves demonstrating the differences in titer between VSV-G- and S(N501Y) protein-pseudotyped LVNPs ($n = 3$ biological replicates). (G) Based on the eGFP titer and p24 ELISA, IU/ng p24 was calculated for the pseudotyped LVNPs. (H) Seven days after transduction, *B2M* KO rates were determined by flow cytometry ($n = 3$ biological replicates). (I) 4×10^4 HEK293T/ACE2$^+$ cells were transduced with serial dilutions of LVNPs targeting *AFF1* ($n = 3$ biological replicates). (J) Schematics of mixed cell sorting experiment. (K) A mixed population consisting of 4×10^4 HEK293T/eGFP$^+$ cells and 4×10^4 HEK293T/ACE2$^+$ cells were treated with 500 ng p24 LVNPs ($n = 3$ biological replicates). Three days after transduction, cells were stained with anti-ACE2-PE and FACS sorted based on receptor expression and eGFP expression. Data are presented as mean (SD). Indel rates were determined by ICE analysis.

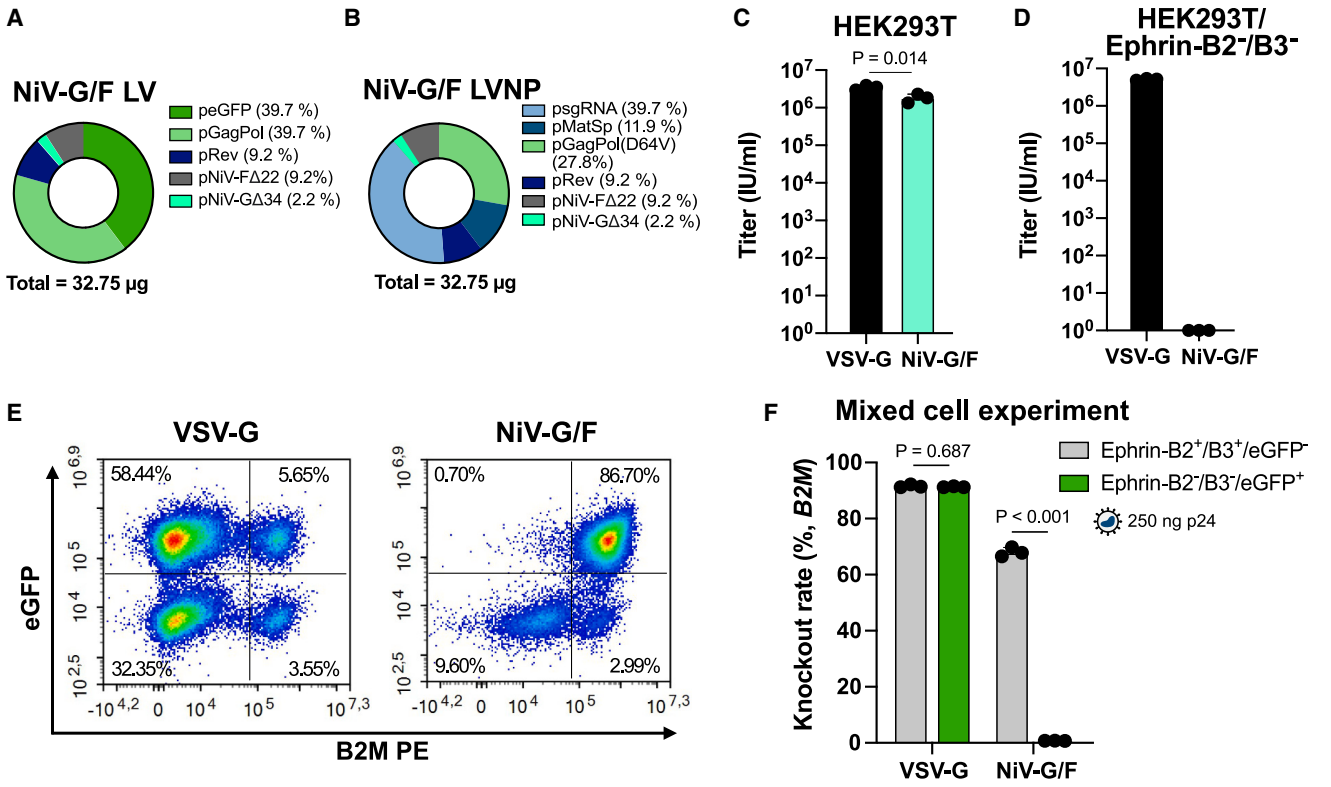

Figure 4. Cell-specific B2M knockout in Ephrin-B2/B3-expressing cells treated with NiV glycoprotein-pseudotyped LVNPs

(A) Plasmid ratios used for production of NiV glycoprotein-pseudotyped LVs. (B) Plasmid ratios used for production of NiV glycoprotein-pseudotyped LVNPs. (C) Viral transduction titers calculated by treating 8×10^4 HEK293T cells with serial dilutions of NiV-G/F-pseudotyped LVs (n = 3 biological replicates). eGFP expression was determined after 3 days using flow cytometry, allowing titers to be determined. (D) Transductional titers determined by treating 8×10^4 HEK293T/Ephrin-B2$^-$/B3$^-$ cells with serial dilutions of NiV-G/F-pseudotyped LVs (n = 3 biological replicates). (E) Example of flow-cytometry-based analysis of mixed cell *B2M* KO experiment. 4×10^4 HEK293T/Ephrin-B2$^-$/B3$^-$/eGFP$^+$ cells were mixed with 4×10^4 HEK293T cells and treated with 250 ng p24 pseudotyped LVNPs. (F) *B2M* KO rates were quantified by flow cytometry 7 days after transduction (n = 3 biological replicates). Data are presented as mean (SD).

Cas9/sgRNA RNPs specifically to a targeted cell population based on pseudotype.

Cell-specific B2M KO in Ephrin-B2/-B3-expressing cells treated with NiV glycoprotein-pseudotyped LVNPs

Like VSV-G, the SARS-CoV-2 S protein mediates uptake of the virus particle through receptor-mediated endocytosis followed by escape from the endosome. To examine the flexibility of LVNP-directed RNP delivery using pseudotyping, we moved on to test Env proteins mediating uptake through membrane fusion (Figure 1). The two NiV glycoproteins, the attachment protein NiV-G and the fusion protein NiV-F, mediate viral uptake through recognition of Ephrin-B2 or -B3 receptors.[44] For production of NiV-G/F glycoprotein-pseudotyped LVs (Figure 4A) and LVNPs (Figure 4B), we used ratios of transfected plasmids that were similar to our standard production with other pseudotypes. However, for the two Env plasmids, pNiV-GΔ34 and pNiV-FΔ22, we employed a 1:5 ratio, which has been shown to increase infection rates compared to a 1:1 ratio.[25,46] As for SARS-CoV-2 S protein, glycoproteins with truncated cytoplasmic tails were used for better incorporation in the viral membrane. In titration experiments, NiV-G/F-pseudotyped LVs showed a clear specificity for cells expressing Ephrin-B2/-B3 receptors, and the titers were comparable in these cells to titers of VSV-G-pseudotyped LVs (Figures 4C, 4D, and S3A). These findings are in agreement with observations by Bender et al.[25] VSV-G-pseudotyped LVs were equally efficient at transducing HEK293T cells and HEK293T cells with double KO of the *EFNB2* and *EFNB3* genes encoding the two receptors (HEK293T/Ephrin-B2$^-$-B3$^-$). In a mixed cell experiment, normal HEK293T cells were mixed with eGFP-expressing HEK293T/Ephrin-B2$^-$/B3$^-$ cells (Figure S1C) and subsequently treated with 250 ng p24 VSV-G- or NiV-G/F-pseudotyped LVNPs targeting the *B2M* locus. Seven days after transduction, cells were stained for β-2 microglobulin and analyzed by flow cytometry (Figures 4E and S3B). Notably, NiV-G/F-pseudotyped LVNPs specifically targeted the eGFP$^-$ HEK293T cells, resulting in 70% KO in this subpopulation, whereas disruption of *B2M* was not evident in HEK293T/Ephrin-B2$^-$/B3$^-$ cells treated with the same LVNPs. In contrast, VSV-G-pseudotyped LVNPs induced >90% *B2M* KO in both subsets of cells (Figure 4F).

SLAM-specific RNP delivery using LVNPs pseudotyped with mutated Edmonston vaccine strain MV-H and MV-F glycoproteins

Next, we wanted to investigate the use of MV glycoproteins for pseudotyped RNP delivery using LVNPs. An SLAM-specific "MV-H/F-SLAM" pseudotype was engineered by combining a Y481N-mutated MV-H[38] with the regular MV-F. During the initial production of MV-H/F- and MV-H/F-SLAM-pseudotyped LVs, distinct changes in producer cell morphology were observed, with the formation of large multinucleated syncytia. To reduce syncytia formation, we created a HEK293T cell line with KO of *CD46* (HEK293T/CD46$^-$) using nucleofection with CRISPR-Cas9 RNPs with two sgRNAs (Figures 5A and S2D). HEK293T/CD46$^-$ producer cells showed a clear reduction in syncytia formation when producing MV-H/F- and MV-H/F-SLAM-pseudotyped LVs compared to CD46-expressing producer cells (Figure 5B). These findings mimic data reported by Ozog and colleagues.[59] We speculated that the reduced syncytia formation could have an advantageous effect on the yield of MV-H/F- and MV-H/F-SLAM-pseudotyped LVs. However, titration experiments in HEK293T cells showed no differences in transductional titers between LVs produced in normal HEK293T cells and HEK293T/CD46$^-$ producer cells (Figures 5C and S1D). In agreement with earlier studies,[60] the transductional titers of MV-H/F-pseudotyped LVs in HEK293T cells were more than 2 logs lower than for VSV-G-pseudotyped LVs (Figure 5C). The gene transfer capacity of MV-H/F- and MV-H/F-SLAM-pseudotyped LVs was similar in HEK293T cells engineered to stably express the SLAM receptor (HEK293T/SLAM$^+$) (Figure 5D). Since MV-H/F-SLAM-pseudotyped LVs did not transduce ordinary HEK293T cells (Figure 5B), this showed specificity for cells expressing SLAM.

For the production of MV-H/F- and MV-H/F-SLAM-pseudotyped LVs and LVNPs, we used higher amounts of Env plasmids than for the previous productions (1:1 between MV-H and MV-F plasmids[37]). Furthermore, by detecting Cas9 in LVNPs with western blotting (Figure 5E and S4A) and ELISA (Figure S4B), we quantified the LVNP load of Cas9 cargo relative to p24 and found that a 1:1 ratio (4.8 μg/4.8 μg) between the packaging constructs pMatSp and pGagPol(D64V) supported the highest level of SpCas9 packaging (Figure 5E). The ratios of production plasmids used for LV and LVNP production are shown in Figures 5F and 5G. To further characterize the LVNPs, we used cryoelectron microscopy (cryo-EM) to achieve high-resolution images of VSV-G- (Figures 5H and S5A) and MV-H/F-SLAM-pseudotyped LVNPs (Figures 5I and S5B). The characteristic cone-shaped HIV-1 capsid was observed after particle maturation. For the MV-H/F-SLAM-pseudotyped LVNPs, the cryo-EM image showed coating of the membrane with Env proteins. Diameters of the LVNPs ranged from 100 to 200 nm.

To validate the specificity of MV-H/F-SLAM-pseudotyped LVNPs, we treated a mixed population of SLAM$^-$/eGFP$^+$ and SLAM$^+$/eGFP$^-$ HEK293T cells with 250 ng p24 VSV-G-, MV-H/F-, or MV-H/F-SLAM-pseudotyped LVNPs carrying Cas9/sgRNA RNPs targeting the *AFF1* locus. The population was then sorted into two subsets, based on eGFP and SLAM expression (Figure S3C). As expected, VSV-G-pseudotyped LVNPs were equally efficient at disrupting the *AFF1* gene in SLAM$^-$ and SLAM$^+$ cells (Figure 5J). MV-H/F-pseudotyped LVNPs were able to deliver Cas9/sgRNA RNPs to cells without the SLAM receptor, resulting in low indel rates, but a preference for cells expressing both CD46 and SLAM receptors was evident, resulting in an *AFF1* gene modification of >80% in the SLAM$^+$ subset of cells. MV-H/F-SLAM-pseudotyped LVNPs did not induce indel formation in SLAM$^-$ cells but specifically targeted SLAM$^+$ cells, leading to indel rates of 60% (Figure 5J). Altogether, these data demonstrate targeted RNP delivery to cells expressing the SLAM receptor using MV-H/F-SLAM-pseudotyped LVNPs.

Efficient DNA modification in primary B cells by MV-H/F- and MV-H/F-SLAM-pseudotyped LVNPs loaded with Cas9/sgRNA RNPs

B cells are highly relevant targets with therapeutic applicability in autoimmune disease, cancer, and infectious disease and are notoriously difficult to transduce using VSV-G-pseudotyped LVs.[37] As MV-H/F-pseudotyped LVs were shown to transduce B cells efficiently,[37] we wanted to investigate the advantages of MV-H/F and MV-H/F-SLAM pseudotyping for LVNP-directed Cas9/sgRNA RNP delivery to primary B cells (Figure S6A). At the start of each experiment, B cells were thawed and seeded on murine MS-5/CD40L$^+$ feeder cells engineered to express CD40 ligand (CD40L) (Figures 6A and S1F). The MS-5/CD40L$^+$ feeder cells were used to culture B cells resulting in CD19$^+$, immunoglobulin (Ig)D$^{+/-}$, CD27$^-$ B cells (Figure 6B). Interleukin (IL)-4 and IL-21 co-stimulation resulted in the down-regulation of IgD expression, and CD27 was also upregulated for a smaller subset of B cells. To understand the potential effect of stimulation on the susceptibility of the cells to LVs carrying the MV-H/F and MV-H/F-SLAM pseudotypes, we examined SLAM expression in CD20$^+$ B cells on the first 3 days of stimulation and used CD20$^-$ feeder cells as a control (Figures 6C and S6B). CD40L stimulation resulted in the gradual upregulation of SLAM (Figure 6D), whereas additional IL-4 and IL-21 stimulation increased SLAM expression levels, quantified by mean fluorescence intensity (MFI) (Figure 6E). We treated 5×10^4 B cells, seeded with 5×10^4 feeder cells, with eGFP-encoding LVs (MOI of 5 IU/cell) and found that B cells were largely unaffected by VSV-G-pseudotyped LVs. In contrast, B cells were highly susceptible to MV-H/F- and MV-H/F-SLAM-pseudotyped LVs, resulting in transfer of the reporter gene to up to >90% of the cells treated with MV-H/F LVs (Figures 6F and S7). IL-4 and IL-21 stimulation led to a further increase in the levels of MV-H/F-SLAM-mediated *EGFP* gene transfer, allowing transduction of >80% of the cells (Figure 6G).

To investigate B cell-targeted LVNP-directed Cas9/sgRNA RNP delivery, 5×10^4 primary B cells were treated with 500 ng p24 LVNPs targeting the *AFF1* gene. No detectable indel formation was observed in B cells treated with VSV-G-pseudotyped LVNPs (Figure 6H). As a control, HEK293T cells were also treated with 100 ng p24 of the same VSV-G-pseudotyped LVNP, resulting in high indel rates (>70%) (Figure S8). In contrast to VSV-G-pseudotyped LVNPs, MV-H/F- and MV-H/F-SLAM-pseudotyped LVNPs induced indel

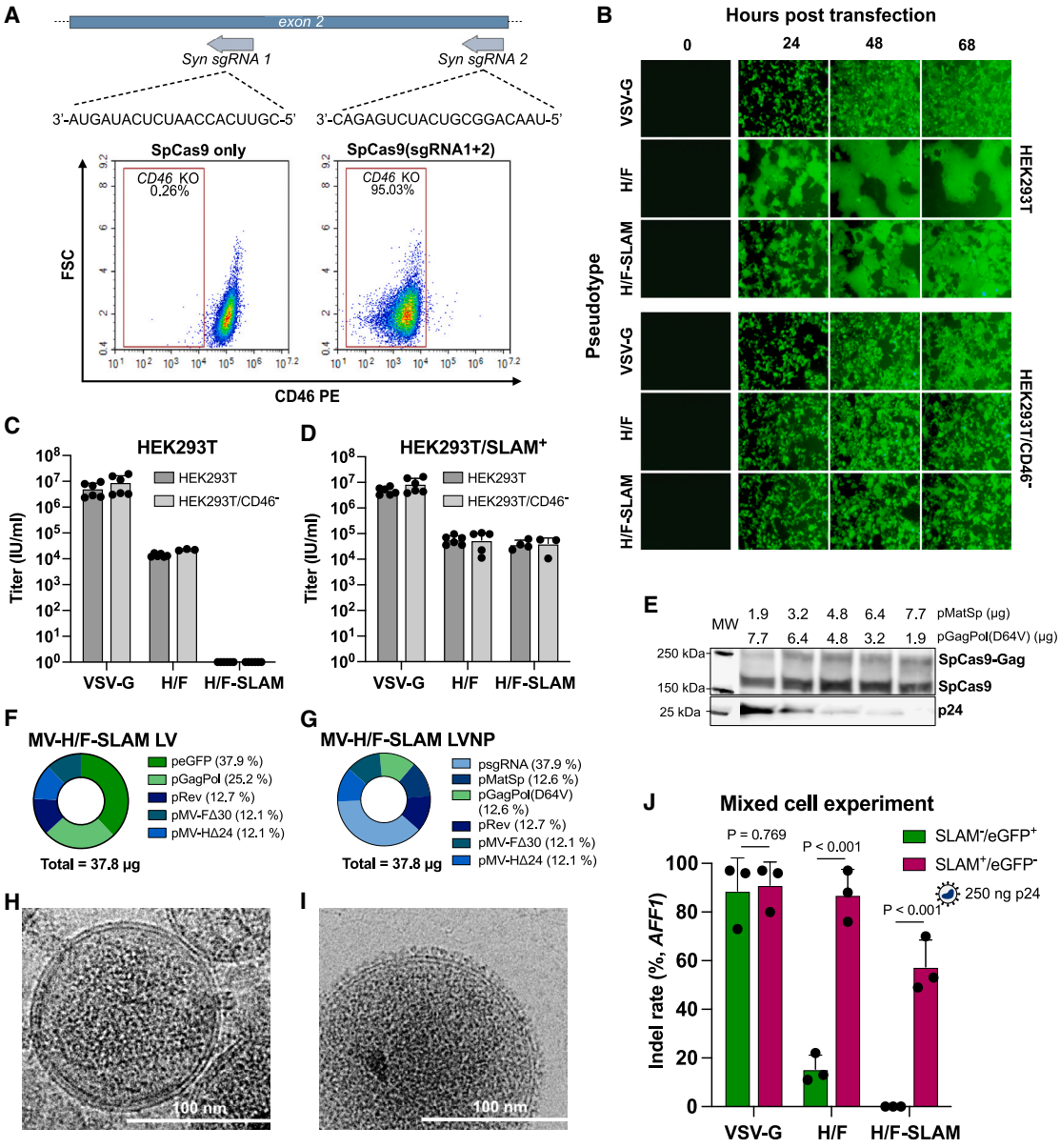

Figure 5. SLAM-specific gene modification using LVNPs pseudotyped with mutated Edmonston MV-H and MV-G glycoproteins

(A) HEK293T cells were electroporated with RNPs consisting of recombinant SpCas9 protein and 2 synthetic sgRNAs for multiplexed DNA cleavage in exon 2 of the *CD46* gene. Flow cytometry analysis showed successful KO in the treated HEK293T population. (B) Fluorescence microscopy showing syncytia formation in HEK293T cells producing MV-H/F- and MV-H/F-SLAM-pseudotyped LVs. Syncytia formation was reduced in HEK293T/CD46^{-} cells. (C) Transductional titers determined by treating 8×10^4 HEK293T cells with serial dilutions of MV-H/F- and MV-H/F-SLAM-pseudotyped LVs (n = 3–6 biological replicates). (D) Transductional titers determined by treating 8×10^4 HEK293T/SLAM^{+} cells with MV-H/F- and MV-H/F-SLAM-pseudotyped LVs (n = 3–6 biological replicates). eGFP expression was determined 3 days after transduction by flow cytometry. (E) Western blot showing relative levels of Cas9 in LVNPs using different plasmid ratios and a clear indication that increased amounts of pGagPol(D64V) resulted in increased amounts of p24, indicative of higher yields. (F) Plasmid ratios used for production of MV-H/F-pseudotyped LVNPs. (G) Plasmid ratios used for production of MV-H/F-SLAM-pseudotyped LVNPs. (H) Representative cryo-EM image of a VSV-G-pseudotyped LVNP. (I) Representative cryo-EM image of an MV-H/F-SLAM-pseudotyped LVNP. (J) 4×10^4 HEK293T/eGFP^{+} cells were mixed with 4×10^4 HEK293T/SLAM^{+} cells before treatment with 250 ng p24 pseudotyped LVNPs (n = 3 biological replicates). After expansion, cells were sorted using FACS based on eGFP expression and SLAM expression. Data are presented as mean (SD). Indel rates were determined by ICE analysis.

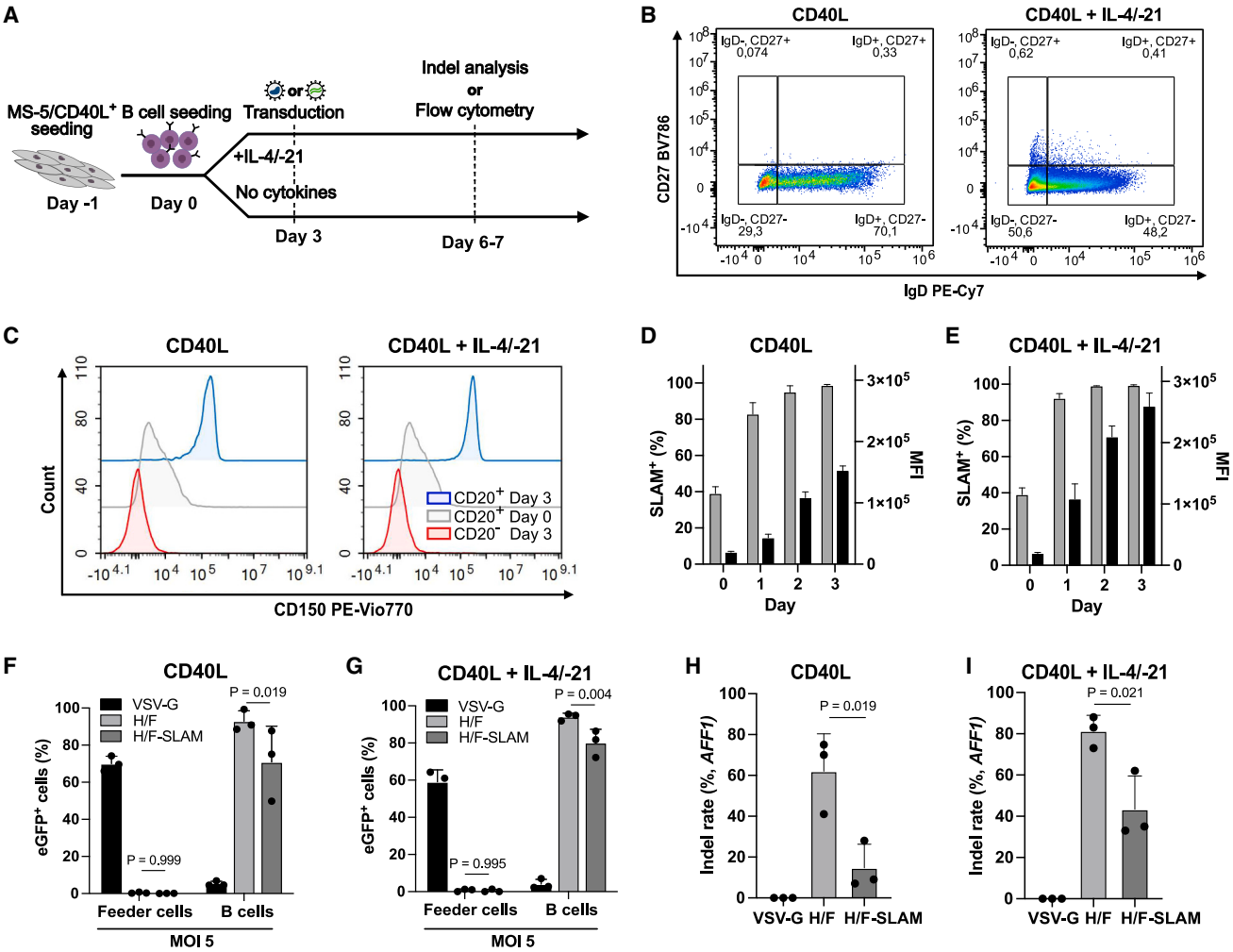

Figure 6. MV-H/F and MV-H/F-SLAM pseudotyping of CRISPR-Cas9/sgRNA-containing LVNPs allows for cell- and gene-targeted DNA cleavage in primary B cells

(A) The workflow for transduction of primary B cells. In half of the experiments, B cells were stimulated by IL-4 and IL-21. (B) Representative B cell profiles at day 6 (donor 1). (C) Representative SLAM expression levels measured by flow cytometry after 3 days of stimulation. CD20 staining was used to discriminate between B cells and feeder cells (donor 1). (D) CD40L stimulation resulted in upregulation of SLAM. Black and gray columns show the MFI and the percentage of SLAM$^+$ cells, respectively (n = 3 biological replicates, donors 1 + 2). (E) Further stimulation with IL-4 and IL-21 resulted in higher MFI, translating to higher levels of SLAM on the cell surface (n = 3 biological replicates, donors 1 + 2). Columns colors as in (D). (F) Pseudotyped LV-mediated *EGFP* gene transfer in B cells. 5 × 10^4 B cells were seeded on 5 × 10^4 feeder cells. B cells were transduced at an MOI of 5 IU/cell (n = 3 biological replicates, donors 1–3). (G) Gene transfer in B cells after IL-4 and IL-21 stimulation. B cells were transduced at an MOI of 5 IU/cell (n = 3 biological replicates, donors 1–3). (H) Indel analysis in B cells after treating 5 × 10^4 B cells with 500 ng p24 pseudotyped LVNPs targeting *AFF1* (n = 3 biological replicates, donors 1 + 2). (I) Stimulation with IL-4 and IL-21 resulted in increased gene modification in B cells treated with MV-H/F- and especially MV-H/F-SLAM-pseudotyped LVNPs (n = 3 biological replicates, donors 1 + 2). Data are presented as mean (SD). Indel rates were determined by ICE analysis.

formation in CD40L-stimulated cells (Figure 6H). In B cells stimulated with CD40L and IL-4/IL-21, increased indel formation was evident for both MV-H/F- and MV-H/F-SLAM-pseudotyped LVNPs, resulting in indel rates reaching >80% and >60%, respectively (Figure 6I). For both CD40L- and CD40L/IL-4/IL-21-stimulated cells, MV-H/F-pseudotyped LVNPs produced markedly higher indel rates than LVNPs pseudotyped with MV-H/F-SLAM. Such a difference between MV-H/F- and MV-H/F-SLAM-pseudotyped LVNPs was not fully mimicked by *EGFP* transfer rates (Figures 6F and 6G), possibly reflecting that *EGFP* transfer by MV-H/F-pseudotyped LVs was almost saturated at an MOI of 5. In conclusion, MV-H/F-SLAM-pseudotyped LVNPs support Cas9/sgRNA RNP delivery to primary B cells, leading to potent targeted DNA cleavage and indel formation in SLAM-expressing B cells stimulated with CD40L, IL-4, and IL-21.

DISCUSSION

Pseudotyping of LVs has been shown to enable receptor-targeted transduction, supporting robust cell-directed gene delivery.[22,36–38,60,61]

However, for gene editing purposes, viral delivery of Cas9- and sgRNA-encoding gene cassettes is potentially associated with an increased risk of off-target cleavage and activation of cellular defense responses due to prolonged or even lifelong expression in recipient cells. To bypass these issues, strategies based on the delivery of Cas9/sgRNA RNPs with transient activity have emerged. Electroporation is a widely used method for the delivery of Cas9/sgRNA RNPs, but this method entails treatment of cells outside the body and is relevant only for *ex vivo* therapies. MLV- and HIV-1-derived particles have been engineered to deliver Cas9/sgRNA RNPs, showing promising results for *ex vivo* applications[16–18] and *in vivo* delivery to mouse liver,[19,62] brain,[19] and eye.[19,21] We recently demonstrated LVNP-mediated *in vivo* delivery of Cas9/sgRNA RNPs to retinal pigment epithelium (RPE) cells in the mouse eye, resulting in gene modification in the *Vegfa* gene (22%).[21] In most studies, such particles were pseudotyped with VSV-G or other pseudotypes with a broad cell tropism to achieve higher transduction efficacy. However, the lack of specificity may increase the risk of unintended editing *in vivo*. Hamilton and co-workers described the use of CD4-specific HIV-1 Env-pseudotyped Cas9-containing particles for targeted co-delivery of Cas9/sgRNA RNPs and transgenes to $CD4^+$ T cells.[18] In a recent paper, the same group further demonstrated the use of such particles for antibody-directed engineering of chimeric antigen receptor (CAR)-T cells.[63] We sought to expand the pseudotyping toolbox for cell-targeted delivery of Cas9/sgRNA RNPs in LVNPs and report the use of several viral glycoproteins, derived from SARS-CoV-2, NiV, and MV, which are novel for the pseudotyping of HIV-1-based protein delivery vehicles.

SARS-CoV-2 S-pseudotyped LVNPs specifically targeted ACE2-expressing cells. One may speculate that such particles could be leveraged for *in vivo* delivery of RNPs to the lung epithelium, targeted at correcting *CFTR* gene variants causing cystic fibrosis.[64] However, immunity resulting from SARS-CoV-2 vaccination represents a restricting factor, possibly requiring the engineering of specialized S protein variants. Others have demonstrated that the pseudotyping of LVs with NiV-G/F results in high titers and efficient transduction of cells expressing Ephrin-B2 or Ephrin-B3, including endothelial cells and a subset of $CD34^+$ cells.[46,47] We report that NiV-G/F-pseudotyped LVNPs specifically deliver Cas9/sgRNA RNPs to Ephrin-$B2^+$/$B3^+$ cells, relevant for genome editing in endothelial cells. Bender et al. described the use of NiV-G-derived glycoprotein fusogens for targeting of LVs toward EpCAM, CD20, and CD8.[25] MV-H-based fusogens have also been developed,[65,66] but MV glycoprotein-pseudotyped LVs are generally produced at lower titers than NiV-G/F-pseudotyped LVs, suggesting that NiV-G-derived fusogens are favorable.

HEK293T/$CD46^-$ producer cells have previously been reported to show reduced syncytia formation and improved production of MV glycoprotein-pseudotyped LVs.[59,67] In our studies, we did observe markedly reduced levels of syncytia formation during LV production in $CD46^-$ producer cells; however, we were not able to document higher LV yields. Despite lower productional yields using MV-derived pseudotypes, MV-H/F-pseudotyped LVs have been demonstrated to be particularly valuable for targeted gene delivery to human primary T and B lymphocytes.[36,37,60] Notably, it has also been reported that MV glycoproteins can be modified to overcome pre-existing immunity.[68,69] We initially showed that Edmonston vaccine strain MV-H/F-pseudotyped LVNPs delivered Cas9/sgRNA RNPs to wild-type HEK293T and engineered SLAM-expressing HEK293T/$SLAM^+$ cells. To narrow the tropism, the acquired affinity for CD46 was removed with a Y481N mutation in the MV-H-encoding plasmid, creating the MV-H/F-SLAM pseudotype.[38] MV-H/F-SLAM-pseudotyped LVNPs specifically targeted SLAM-expressing cells in a population of cells consisting of both $SLAM^+$ and $SLAM^-$ cells, demonstrating that LVNPs support targeted DNA modification in a defined subset of cells.

Relative to T cells, B cells have received less attention for cell-based therapies. However, the ability to secrete large amounts of specific antibodies makes the B cell lineage an important target for cell-targeted gene therapies.[70] In agreement with others, we show efficient gene delivery to activated primary B cells using MV-H/F-pseudotyped LVs.[67] In addition, LVs pseudotyped with the engineered MV-H/F-SLAM pseudotype facilitated high levels of SLAM-specific gene transfer in activated B cells. CRISPR-Cas9-mediated gene modification in primary human B cells has primarily been achieved using electroporation of RNP complexes and AAV vectors for subsequent HDR donor delivery. Moffett and co-workers described the engineering of primary human and murine B cells for expression of pathogen-specific antibodies with a protecting effect against infection.[54] Additionally, Nahmad et al. reported that engineered B cells retained abilities for immunological memory, isotype switching, and clonal expansion.[55] Gutierrez-Guerrero et al. achieved modest multiplexed editing (12%–15%) in the *WASP* gene in activated primary B cells after using MLV- and HIV-based VLPs co-pseudotyped with VSV-G and baboon Env (BaEV) glycoproteins.[17] Luo and co-workers used BaEV-pseudotyped integrase-defective LVs (IDLVs) to deliver vector RNA encoding Cas9 and sgRNA or carrying the HDR donor for the engineering of B cells that were capable of differentiating into anti-PD-1 antibody-expressing plasma cells both *in vitro* and *in vivo*.[71] Using MV-H/F-pseudotyped LVNPs, we demonstrated the delivery of Cas9/sgRNA RNPs, reaching indel rates of >80% in primary B cells stimulated with CD40L, IL-4, and IL-21. LVNPs pseudotyped with the engineered SLAM-specific MV-H/F-SLAM pseudotype also resulted in highly potent indel formation in activated B cells. MV-H/F-SLAM has a narrow tropism compared to MV-H/F, making it more suitable for *in vivo* gene engineering of lymphocytes, including B cells. Previous studies found that stable MV-H/F-mediated LV gene delivery to quiescent lymphocytes required binding to both SLAM and CD46 receptors, which could challenge LVNP-directed protein delivery as well.[38,72] Our results show that B cell SLAM expression levels are upregulated in response to CD40L, IL-4, and IL-21 stimulation, which enables higher MV-H/F- and especially MV-H/F-SLAM-mediated delivery of Cas9/sgRNA RNPs. This highlights the importance of SLAM expression levels for targeted gene editing using these specific pseudotypes but also suggests that susceptibility to MV-H/F-SLAM LVNP-mediated gene modification might differ between

B cell activation states. As an alternative approach, an engineered NiV-G-derived fusogen targeting CD20 could potentially direct LVNP-mediated Cas9/sgRNA RNP delivery specifically to $CD20^+$ B cells.

Pseudotyped LVNPs loaded with Cas9/sgRNA RNPs are currently one of few approaches allowing cell-targeted delivery of "ready-to-work" gene editing complexes. So far, such particles allow delivery of RNPs, targeted DNA cleavage, and indel formation but do not support HDR-based gene editing. To introduce a specific edit sequence, co-transduction with an AAV vector carrying a donor sequence could potentially facilitate HDR. Alternatively, engineered "all-in-one" LVNPs carrying both Cas9/sgRNA RNPs as well as vector RNA that undergoes reverse transcription and may then serve as a donor template may ultimately enable cell-targeted gene editing in primary human B cells *in vivo*. Notably, it has been reported that Env-specific B cell receptors can direct LV tropism *in vivo*.[73]

In 2023, we reported on the capacity of VSV-G-pseudotyped LVNPs to incorporate and deliver base and prime editors.[21] An et al. recently established VSV-G-pseudotyped engineered virus-like particles (eVLPs) as vehicles for the delivery of prime editors *in vivo*.[74] The use of other pseudotypes, like those presented in this study, opens new avenues for implementing the LVNP delivery technology for gene editing in a targeted population of cells without generating double-stranded DNA breaks or supplying a DNA donor sequence.

MATERIALS AND METHODS

Cell cultures

HEK293T (Lenti-X 293T) cells (Takara Bio, cat. #632180, San Jose, CA, USA) were cultured in Dulbecco's modified Eagle medium (DMEM) (Sigma-Aldrich, cat. #D6429, St. Louis, MO, USA) supplemented with 5% fetal bovine serum (FBS) (Sigma-Aldrich, cat. #F7524), 100 U/mL penicillin, and 100 μg/mL streptavidin (penicillin/streptavidin [P/S]) (Gibco, cat. #15140122, Waltham, MA, USA). Cells were passaged at 80%–90% confluency using 0.05% trypsin (SAFC, cat. #59417C, St. Louis, MO, USA). MS-5 cells (DSMZ, cat. #ACC 441, Braunschweig, Germany), SupT1 cells, and primary B cells were cultured in RPMI 1640 (Sigma-Aldrich, cat. #R8758) supplemented with 10% FBS and 1% P/S. For engineered receptor-expressing cell lines, 5 μg/mL puromycin (Gibco, cat. #A1113803) or 5 μg/mL blasticidin S (Gibco, cat. #A1113903) was added to the media for selection depending on the antibiotic resistance gene in the integrated gene cassette. Cells were cultured at 37°C with 5% CO_2.

Flow cytometry and fluorescence-activated cell sorting

Between 1×10^5 and 1×10^7 cells were stained in 50 μL fluorescence-activated cell sorting (FACS) buffer (phosphate-buffered saline [PBS], 1% BSA, 2.5 mM EDTA, 25 mM HEPES) using recommended antibody concentrations or less for titrated antibodies. If necessary, cells were fixated in 0.9% paraformaldehyde buffer for 30 min at room temperature (RT). A NovoCyte 3000 or NovoCyte Quanteon 4025 (Agilent, Santa Clara, CA, USA) was used for flow cytometry experiments. For sorting experiments, a Bigfoot Cell Sorter (Invitrogen, Waltham, MA, USA) was used for sorting live BSL-2 samples, and FACSAria III (BD Biosciences, San Jose, CA, USA) was used for fixated samples. All instruments were maintained by the FACS core staff at the Department of Biomedicine Aarhus University. FlowJo and NovoExpress software were used for flow analysis. A list of antibodies is provided in Table S2.

B cell purification

B cells were purified from buffy coats obtained from anonymous healthy blood donors from the Aarhus University Hospital Blood Bank using the StraightFrom Buffy Coat CD19 MicroBead purification kit (Miltenyi Biotec, cat. #130-114-974, Bergisch Gladbach, Germany) following the manufacturer's instructions. Purification was subsequently assessed by flow cytometry using an anti-CD19 BV421 antibody (BD Biosciences, cat. #562440, Franklin Lakes, NJ, USA) together with several other antibodies from BD Biosciences: anti-CD20 Alexa Fluor 700 (cat. #560631), anti-CD24 PE-CF594 (cat. #562405), anti-CD27 BV786 (cat. #563327), anti-CD38 APC (cat. #555462), and anti-IgD PE-Cy7 (cat. #561314). Staining was performed in BD Brilliant Horizon stain buffer (BD Biosciences, cat. #563794) supplemented with Fc block (BD Biosciences, cat. #564220). Cells were frozen in cryotubes in FBS supplemented with 10% DMSO (Supelco, cat. #1.02950, St. Louis, MO, USA).

Engineering of KO cell lines

HEK293T/Ephrin-B2$^-$/B3$^-$

For production of Ephrin-B2/B3 KO cells, sgRNAs were designed to target the coding regions of Ephrin-B2 (EFNB2) and Ephrin-B3 (EFNB3) genes (Table S1) and synthesized by Integrated DNA Technologies (IDT) (Coralville, IA, USA) with 2′ O-methyl analogs on the first and last three bases. All sgRNAs were screened by RNP electroporation into HEK293T cells using an 4D-Nucleofector (core and x-unit) (Lonza, Basel, Switzerland) and Cell Line Nucleofector Kit V (Lonza, cat. #VCA-1003) using the IDT Alt-R CRISPR-Cas9 System according to the manufacturer's instructions. Briefly, 120 pmol of each sgRNA was complexed with 100 pmol Alt-R Cas9 V3 recombinant enzyme (IDT, cat. #1081059) in a final volume of 5 μL for 20 min. Subsequently, each RNP was diluted with 100 μL of Nucleofector Solution V and used to resuspend a 1×10^6 pellet of cells, which were immediately transferred to a nucleofection cuvette and nucleofected using program Q-01. 500 μL of medium was used to transfer the transfected cells to a fresh 6-well plate. Four days later, cells were collected and their genomic DNA extracted using Lucigen QuickExtract (LGC Biosearch Technologies, cat. #QE09050, Teddington, UK). The targeted regions were amplified by PCR and Sanger sequenced at Genewiz (Leipzig, Germany). The chromatograms of each transfected sample were compared to a transfected sample using TIDE[75] to assess the overall editing efficiency. The best sgRNAs, EFNB3_sgRNA3 and EFNB2_sgRNA8, were then mixed and nucleofected together into new wild-type HEK293T cells following the same protocol. After 4 days, cells were passaged and seeded at a limiting dilution. Single-cell-containing wells were identified. To functionally screen for full double EFNB2/EFNB3 KO clones, a replica 24-well plate was transduced with NiV-G/F-pseudotyped

LVs carrying a GFP expression cassette. Clones that had less than 0.2% GFP positivity were selected as full KO clone candidates. Full double KO was confirmed by genetic characterization via PCR and TIDE analysis.

HEK293T/CD46^{-}

A total of 3.2 μg of CD46_sgRNA1 and CD46_sgRNA2 (Table S1), designed and ordered at Synthego (Redwood City, CA, USA), was mixed with 6 μg of Alt-R Cas9 V3 recombinant SpCas9 enzyme (IDT, cat. #1081059) and incubated for 15 min at RT for components to form RNP complexes. Then, 8×10^5 HEK293T cells were electroporated with the RNP complexes in 20 μL P3 Primary Cell Nucleofector buffer (Lonza, cat. #V4XP-3032) using program CN-114 on the Lonza 4D-Nucleofector. CD46 KO was verified by flow cytometry using a NovoCyte flow cytometer (Agilent) after staining with an anti-CD46 antibody (Table S2).

Plasmids

All plasmids that were used in this study (plasmids that were generated for this study and plasmids published elsewhere) are listed in Table S3. Plasmids pcDNA3.1_spike_del19 (Addgene plasmid #155297; http://n2t.net/addgene:155297; RRID: Addgene_155297) and pLENTI_hACE2_puro (Addgene plasmid #155295; http://n2t.net/addgene:155295; RRID: Addgene_155295) were gifts from Raffaele De Francesco. The point mutation in pcDNA3.1_spike_del19(N501Y) was made using NEBuilder HiFi DNA Assembly Master Mix (New England Biolabs, cat. #NEB-E5520S, Ipswich, MA, USA). pCG-HΔ24 and pCG-FΔ30 were gifts from Els Verhoeyen. The point mutation in pCG-HΔ24(Y481N) was also made using NEBuilder HiFi DNA Assembly Master Mix (New England Biolabs). pNiV-FΔ22 and pNiV-GΔ34 plasmids were supplied by Sana Biotechnology (Seattle, WA, USA). Plenti-EFS-EGFP-P2A-Blast was used to generate the eGFP$^+$ target cells used in the mixed cell populations. pLX304-SLAMf1 was purchased from Harvard Plasmid Bank and used for the cloning of pCCL-PGK-SLAMf1-P2A-Blast. pCCL-PGK-CD40LG-IRES-Puro was constructed by linearization of pCCL-PGK-MCS-IRES-Puro using BamHI (Thermo Scientific, cat. #FD0055, Waltham, MA, USA) and insertion of a fragment amplified from cd40lg-in-pcr4-topo obtained from Harvard Plasmid Bank. The assembly of constructs with fragments was performed using NEBuilder HiFi DNA Assembly Master Mix (New England Biolabs) according to the manufacturer's instructions. Plenti-EFS-EGFP-P2A-Blast was cloned by digesting lentiCas9-Blast with AgeI and BamHI. *EGFP* was amplified from pCCL-PGK-EGFP, and the resulting fragment and digested backbone were assembled using NEBuilder HiFi DNA Assembly Master Mix (New England Biolabs). The primers used for cloning are listed in Table S4.

LV production

VSV-G-pseudotyped LVs were produced in HEK293T cells. 4×10^6 cells were seeded in 10 cm dishes. The following day, the medium was exchanged 1 h before the cells were transfected with 13 μg pCCL-PGK-EGFP (transfer plasmid; pEGFP), 13 μg pMDLg/pRRE (GagPol), 3.75 μg pMD2.G (VSV-G), and 3 μg pRSV-Rev (Rev) using 50 μL 2.5 M $CaCl_2$ and 500 μL 2×HBS solution. For pseudotyping with SARS-CoV-2 S protein, 3.75 μg pcDNA3.1_spike_del19 or pcDNA3.1_spike_del19(N501Y) was used. For the production of LVs pseudotyped with NiV Env protein, 3 μg pNiV-FΔ22 and 0.75 μg pNiV-GΔ34 were used. For the production of MV- and MV-H/F-SLAM-pseudotyped LVs, producer cells were transfected with 14.33 μg pCCL-PGK-EGFP (transfer plasmid), 9.55 μg pMDLg/pRRE (GagPol), 4.58 μg pCG-HΔ24 or pCG-HΔ24(Y481N), 4.58 μg pCG-FΔ30, and 4.78 μg pRSV-Rev using 91.7 μL 2.5 M $CaCl_2$ and 750 μL 2×HBS solution. The next day, the medium was exchanged for 9 mL fresh DMEM. The following day, vectors were harvested, filtered using a 0.45 μm filter, and stored in the fridge as an unconcentrated virus or ultracentrifuged through a 20% sucrose cushion at 25,000 rpm, 4°C, for 2 h. Ultracentrifuged virus pellets were resuspended in PBS (Gibco) overnight.

Transductional titer and MOI of LVs

Tranductional titers (defined as IU/mL) of pseudotyped LVs were determined from titration experiments based on the transfer of vector RNA carrying the *EGFP* gene driven by the PGK promoter (CCL/PGK-EGFP). Recipient cells were seeded in the presence of LVs in a 12-well plate using 500 μL of serial dilutions of unconcentrated preparations of LVs. Three days after transduction, the percentage of eGFP$^+$ cells was determined by flow cytometry. Dilutions resulting in 1%–20% eGFP$^+$ cells were used to calculate the titer using the following equation:

$$\text{titer} = \left(\frac{\text{total cell number} \times \%\ \text{eGFP}^+\ \text{cells in decimals}}{\text{volume}}\right) \times \text{dilution factor.}$$

Determination of the transductional titers allowed the MOI (defined as IU/cell) to be estimated for individual experiments.

Engineering of receptor-expressing target cells and feeder cells

HEK293T/ACE2$^+$

2×10^5 HEK293T cells were treated with LVs carrying transfer vector RNA derived from pLENTI_hACE2_puro (Table S3). Selection was achieved by treating the transduced cells with puromycin (5 μg/mL). Clones were obtained by isolating the colonies after seeding the cells at a very low density in p10 dishes. The ACE2 expression level was determined by flow cytometry.

HEK293T/eGFP$^+$

2×10^5 HEK293T cells were treated with LVs carrying vector RNA derived from plenti-EFS-EGFP-P2A-Blast. Selection was achieved by treating the transduced cells with blasticidin S (5 μg/mL). Clones were isolated and analyzed for expression of eGFP protein by flow cytometry.

HEK293T/SLAM$^+$

2×10^5 HEK293T cells were treated with LVs carrying transfer vector RNA expressed from pCCL-PGK-SLAMf1-P2A-Blast. Selection was

achieved by treating the transduced cells with blasticidin S (5 μg/mL). Clones were isolated and analyzed for SLAM expression by flow cytometry.

MS-5/CD40L$^+$

1×10^5 MS-5 cells (DSMZ, cat. #ACC 441) were treated with LVs carrying the transfer vector RNA derived from pCCL-PGK-CD40LG-IRES-Puro. Subsequent selection with puromycin (1 μg/mL) resulted in a population of CD40L-expressing MS-5 feeder cells.

Production of LVNPs

VSV-G-pseudotyped LVNPs were produced in HEK293T cells as previously described.[21] In brief, 4×10^6 cells were seeded in 10 cm plates. The following day, the medium was exchanged 1 h before cells were transfected with 13 μg pU6-sgRNA-OptBB2-CBh-EGFP (sgRNA), 3.9 μg pSpCas9-PH-gagpol-D64V (MatSp), 9.1 μg pMDLg/pRRE-D64V (pGagPol(D64V)), 3.75 μg pMD2.G (VSV-G), and 3 μg pRSV-Rev (Rev) using 50 μL 2.5 M $CaCl_2$ and 500 μL 2×HBS solution. For pseudotyping with SARS-CoV-2 S and NiV glycoproteins, the same total amount of Env plasmids was used as described for LV production (3.75 μg pcDNA3.1_spike_del19(N501Y) and 3 μg pNiV-FΔ22/0.75 μg pNiV-GΔ34, respectively). For standard MV- and MV-H/F-SLAM-pseudotyped LVNPs, 14.33 μg pU6-sgRNA-OptBB2-CBh-EGFP (sgRNA), 4.8 μg pSpCas9-PH-gagpol-D64V (MatSp), 4.8 μg pMDLg/pRRE-D64V (pGagPol(D64V)), 4.58 μg pCG-HΔ24 or pCG-HΔ24(Y481N), 4.58 μg pCG-FΔ30, and 4.78 μg pRSV-Rev (Rev) were used in a total volume of 658.3 μL, with the subsequent addition of 91.7 μL 2.5 M $CaCl_2$ and mixing with 750 μL 2×HBS solution. LVNPs were harvested and ultracentrifuged as described for LVs. For all preparations of LVNPs, the transfection cocktail contained the two packaging constructs pSpCas9-PH-gagpol-D64V (MatSp) and pMDLg/pRRE-D64V (pGagPol(D64V)), the latter of which did not contain the fusion domain. We routinely generated SpCas9/sgRNA-loaded LVNPs carrying both normal Gag/GagPol and SpCas9-fused Gag/GagPol since the combined yield and performance of such mixed particles is higher than if the particles do not carry normal Gag/GagPol.[21] All Pol variants carry the D64V-mutated integrase, rendering the integrase inactive, as LVNP function does not rely on integrase activity. LVNPs carrying both Cas9/sgRNA RNPs and vector RNA were produced essentially as described above. Briefly, 4×10^6 HEK293T cells were seeded in p10 dishes. The following day, the cells were transfected with 5.2 μg pU6-sgRNA-OptBB2-CBh-EGFP (sgRNA), 7.8 μg pCCL-PGK-EGFP (transfer plasmid), 3.9 μg pSpCas9-PH-gagpol-D64V (MatSp), 9.1 μg pMDLg/pRRE-D64V (pGagPol(D64V)), 3.75 μg pMD2.G (VSV-G), and 3 μg pRSV-Rev (Rev) using 50 μL 2.5 M $CaCl_2$ and 500 μL 2×HBS solution. For pseudotyping with SARS-CoV-2 S(N501Y), 3.75 μg pcDNA3.1_spike_del19(N501Y) was used instead of pMD2.G. LVNPs were stored in 50–250 μL aliquots at −70°C and only thawed once.

LVNP quantification, analysis, and treatment of cells

P24 ELISA (XpressBio, cat. #XB-1000, Frederick, MD, USA) was used to evaluate LVNP quantity. Cas9 ELISA (XpressBio, cat. #Cas9-1000) was used to analyze Cas9 amounts using the manufacturer's instructions. 8×10^4 recipient cells were seeded in the presence of LVNPs in a total volume of 500 μL using 15–500 ng of p24 LVNPs quantified by ELISA. The day after treatment, the medium was replaced with fresh medium for adherent cells and supplemented with 500 μL fresh medium for suspension cells. Three to four days after treatment, cells were harvested and lysed for analysis of genetic modifications. For *B2M* KO, cells were cultured for a week before flow cytometry was used to determined surface expression levels based on staining with an anti-B2M-PE antibody (BioLegend, cat. #316305, San Diego, CA, USA).

LVNP treatment of primary B cells

For the treatment of primary B cells with LVNPs, 5×10^4 MS-5/CD40L$^+$ feeder cells were seeded in 48-well plates 1 day prior to treatment. B cells were thawed and counted the following day, and 5×10^4 B cells were seeded on the feeder cell monolayer in a total of 300 μL RPMI 1640 supplemented with 10% FBS and 1% P/S. For IL-4 (PeproTech, cat. #200-04, Cranbury, NJ, USA) and IL-21 (PeproTech, cat. #200-21) stimulation, a concentration of 5 ng/mL was used for each of the cytokines. After 3 days of co-culture, LVs or LVNPs were added, and an additional medium was supplied to reach a total volume of 500 μL. The following day, 500 μL of fresh culture medium was added to each well with or without IL-4 and IL-21.

DNA extraction and indel analysis

Cells were lysed for 2 h at 55°C using chorion villus lysis buffer (10 mM Tris-HCl, 1 mM EDTA, 150 mM NaCl, 0.5% SDS) and 1% proteinase K (Thermo Scientific, cat. #EO0491). Proteins were precipitated using 6M NaCl, and ice-cold absolute ethanol was used to extract the DNA. PCR was performed using Phusion High-Fidelity DNA Polymerase Master Mix (Thermo Scientific, cat. #F531L) using the primers (from Tag Copenhagen or IDT) listed in Table S5. 5 μL of the PCR reaction was treated with 0.5 μL FastAP Thermosensitive Alkaline Phosphatase (Thermo Scientific, cat. #EF0651) and 0.5 μL Exonuclease I (New England Biolabs, cat. #NEB-M0293S) in a total volume of 18 μL at 37°C for 15 min. Alternatively, the PCR product was visualized on a 1% agarose gel, and the DNA was extracted using E.Z.N.A. Gel Extraction Kit (Omega Bio-tek, cat. #D6294-02, Norcross, GA, USA). Samples were sequenced by Sanger sequencing (Eurofins Genomics, Ebersberg, Germany). Indels were analyzed using Synthego's Interference of CRISPR Edits (ICE) analysis tool.[76]

Western blot analysis

LVNPs were analyzed for relative amounts of p24 and FLAG-tagged SpCas9 amounts using western blotting. The samples were denatured for 5 min at 100°C in the presence of 1× XT sample buffer (Bio-Rad, cat. #1610791, Hercules, CA, USA) and 1× XT reducing agent (Bio-Rad, cat. #1610792). SDS-PAGE was used to separate proteins on a 4%–15% Criterion TGX precast gel (Bio-Rad, cat. #5671084), followed by blotting onto a PVDF membrane (Bio-Rad, cat. #1704157). The membrane was blocked for 1 h using 5% skim milk (Sigma-Aldrich) in TBS/0.05% Tween 20 solution. Subsequently, the membrane was incubated with a 1:5,000 dilution of

mouse anti-FLAG antibody (Sigma-Aldrich, cat. #F3165) overnight at 4°C. The following day, the blot was washed and incubated with a 1:10,000 dilution of goat anti-mouse HRP antibody (Agilent Dako, cat. #P0447) and subsequently treated with Clarity Western ECL Substrate (Bio-Rad, cat. #1705060) before chemiluminescence visualization. The membrane was stripped using Restore PLUS Western Blot Stripping Buffer (Thermo Scientific, cat.# 46430) and then incubated with a 1:1,000 dilution of rabbit anti-p24 antibody (R&D Systems, cat. #MAB9539, Minneapolis, MN, USA). The following day, the blot was washed, incubated with a 1:10,000 dilution of goat anti-rabbit HRP antibody (Agilent Dako, cat. #P0448) for 1 h, and visualized as previously described.

Cryo-EM

Samples were prepared for cryo-EM using a Leica GP2. A 3 μL sample was applied to 2/1 200 mesh C-flat grids (Protochips) and blotted for 3 s before plunging into liquid ethane. Grids were treated in a GloQube (Quorum) glow discharge system for 45 s at 15 mA. The samples were imaged on a Cs-corrected Titan Krios 300 kV transmission electron microscope (TEM; Thermo Scientific) at 165 kx, corresponding to a pixel size of 0.835 Å/px on a Gatan BioQuantum K2 direct detector camera operating in counted mode and a slit width of 20 eV. Cs correction using CEOS software measured Cs = 4 μm before the final correction of astigmatism after inserting a 100 μm objective aperture. New gain reference and tuning of the energy filter were performed prior to data collection. Data collection was set up using EPU 2.12 for a total dose of 60 e/Å2 per 7.6 s exposure in 38 frames. A target defocus of −1.6 to −2.0 μm was used. 325 movies were collected from the VSV-G sample and 1,644 for the MV-H/F-SLAM sample. The movies were motion corrected using Warp (www.warpem.com). EM sample preparation and imaging was performed at the EMBION cryo-EM facility (https://embion.au.dk) at iNANO, Aarhus University.

Statistical analysis

Statistical analysis was performed using GraphPad Prism software. For grouped data, two-way ANOVA with Tukey's multiple comparison test was applied to compare group means with every other mean. The unpaired t test was applied to compare the means of two independent groups.

DATA AND CODE AVAILABILITY

The data underlying this article are available within the article and its online material. Original plasmids are available upon request from the corresponding author and will be made available through Addgene.

ACKNOWLEDGMENTS

A sponsored research agreement between Aarhus University and Sana Biotechnology, Inc., provided partial funding for this work, which was also supported by the Graduate School of Health, Aarhus University, and project grants from the Innovation Fund Denmark (PASCAL-MID, 8056-00010A) and Novo Nordisk Foundation (NNF22OC0080684). Furthermore, funding for the Bigfoot Cell Sorter was provided by the Carlsberg Foundation (personal grant to J.G.M.; ID CF21-0363). We acknowledge the FACS Core Facility at Aarhus University for assistance with flow cytometry and FACS.

AUTHOR CONTRIBUTIONS

Conceptualization, I.H.N. and J.G.M.; methodology, J.G.M., I.H.N., and J.V.S.; investigation, I.H.N., A.B.R., J.H.J., E.A.T., A.R., F.N., C.T.M., and A.B.; writing – original draft, I.H.N. and J.G.M.; writing – review & editing, I.H.M. and J.G.M.; project administration, I.H.N. and J.G.M.; funding acquisition, J.G.M.; resources, J.G.M., J.V.S., S.E.D., and T.B.; supervision, J.G.M., J.V.S., and S.E.D.; formal analysis, I.H.N.; visualization, I.H.N.

DECLARATION OF INTERESTS

J.G.M. is a member of the scientific advisory board of Nvelop Therapeutics. The company was not involved in the present study.

SUPPLEMENTAL INFORMATION

Supplemental information can be found online at https://doi.org/10.1016/j.omtn.2024.102318.

REFERENCES

1. Barrangou, R., Fremaux, C., Deveau, H., Richards, M., Boyaval, P., Moineau, S., Romero, D.A., and Horvath, P. (2007). CRISPR provides acquired resistance against viruses in prokaryotes. Science *315*, 1709–1712.
2. Jinek, M., Chylinski, K., Fonfara, I., Hauer, M., Doudna, J.A., and Charpentier, E. (2012). A programmable dual-RNA-guided DNA endonuclease in adaptive bacterial immunity. Science *337*, 816–821.
3. Wiedenheft, B., Sternberg, S.H., and Doudna, J.A. (2012). RNA-guided genetic silencing systems in bacteria and archaea. Nature *482*, 331–338. https://doi.org/10.1038/nature10886.
4. Mali, P., Esvelt, K.M., and Church, G.M. (2013). Cas9 as a versatile tool for engineering biology. Nat. Methods *10*, 957–963. https://doi.org/10.1038/nmeth.2649.
5. Young, L.S., Searle, P.F., Onion, D., and Mautner, V. (2006). Viral gene therapy strategies: from basic science to clinical application. J. Pathol. *208*, 299–318. https://doi.org/10.1002/path.1896.
6. Zufferey, R., Dull, T., Mandel, R.J., Bukovsky, A., Quiroz, D., Naldini, L., and Trono, D. (1998). Self-Inactivating Lentivirus Vector for Safe and Efficient In Vivo Gene Delivery. J. Virol. *72*, 9873–9880.
7. Naldini, L., Blömer, U., Gallay, P., Ory, D., Mulligan, R., Gage, F.H., Verma, I.M., and Trono, D. (1996). In vivo gene delivery and stable transduction of nondividing cells by a lentiviral vector. Science *272*, 263–267.
8. Wolff, J.H., and Mikkelsen, J.G. (2022). Delivering genes with human immunodeficiency virus-derived vehicles: still state-of-the-art after 25 years. J. Biomed. Sci. *29*, 79. https://doi.org/10.1186/s12929-022-00865-4.
9. Aoki, T., Miyauchi, K., Urano, E., Ichikawa, R., and Komano, J. (2011). Protein transduction by pseudotyped lentivirus-like nanoparticles. Gene Ther. *18*, 936–941. https://doi.org/10.1038/gt.2011.38.
10. Izmiryan, A., Basmaciogullari, S., Henry, A., Paques, F., and Danos, O. (2011). Efficient gene targeting mediated by a lentiviral vector-associated meganuclease. Nucleic Acids Res. *39*, 7610–7619. https://doi.org/10.1093/nar/gkr524.
11. Cai, Y., Bak, R.O., Krogh, L.B., Staunstrup, N.H., Moldt, B., Corydon, T.J., Schrøder, L.D., and Mikkelsen, J.G. (2014). DNA transposition by protein transduction of the piggyBac transposase from lentiviral Gag precursors. Nucleic Acids Res. *42*, e28. https://doi.org/10.1093/nar/gkt1163.
12. Cai, Y., Bak, R.O., and Mikkelsen, J.G. (2014). Targeted genome editing by lentiviral protein transduction of zinc-finger and TAL-effector nucleases. Elife *3*, e01911. https://doi.org/10.7554/eLife.01911.
13. Cai, Y., Laustsen, A., Zhou, Y., Sun, C., Anderson, M.V., Li, S., Uldbjerg, N., Luo, Y., Jakobsen, M.R., and Mikkelsen, J.G. (2016). Targeted, homology-driven gene insertion in stem cells by ZFN-loaded 'all-in-one' lentiviral vectors. Elife *5*, e12213. https://doi.org/10.7554/eLife.12213.
14. Choi, J.G., Dang, Y., Abraham, S., Ma, H., Zhang, J., Guo, H., Cai, Y., Mikkelsen, J.G., Wu, H., Shankar, P., and Manjunath, N. (2016). Lentivirus pre-packed with Cas9 protein for safer gene editing. Gene Ther. *23*, 627–633. https://doi.org/10.1038/gt.2016.27.
15. Skipper, K.A., Nielsen, M.G., Andersen, S., Ryø, L.B., Bak, R.O., and Mikkelsen, J.G. (2018). Time-Restricted PiggyBac DNA Transposition by Transposase Protein

Delivery Using Lentivirus-Derived Nanoparticles. Mol. Ther. Nucleic Acids *11*, 253–262. https://doi.org/10.1016/j.omtn.2018.02.006.

16. Indikova, I., and Indik, S. (2020). Highly efficient 'hit-and-run' genome editing with unconcentrated lentivectors carrying Vpr.Prot.Cas9 protein produced from RRE-containing transcripts. Nucleic Acids Res. *48*, 8178–8187. https://doi.org/10.1093/nar/gkaa561.

17. Gutierrez-Guerrero, A., Abrey Recalde, M.J., Mangeot, P.E., Costa, C., Bernadin, O., Périan, S., Fusil, F., Froment, G., Martinez-Turtos, A., Krug, A., et al. (2021). Baboon Envelope Pseudotyped "Nanoblades" Carrying Cas9/gRNA Complexes Allow Efficient Genome Editing in Human T, B, and CD34(+) Cells and Knock-in of AAV6-Encoded Donor DNA in CD34(+) Cells. Front. Genome Ed. *3*, 604371. https://doi.org/10.3389/fgeed.2021.604371.

18. Hamilton, J.R., Tsuchida, C.A., Nguyen, D.N., Shy, B.R., McGarrigle, E.R., Sandoval Espinoza, C.R., Carr, D., Blaeschke, F., Marson, A., and Doudna, J.A. (2021). Targeted delivery of CRISPR-Cas9 and transgenes enables complex immune cell engineering. Cell Rep. *35*, 109207. https://doi.org/10.1016/j.celrep.2021.109207.

19. Banskota, S., Raguram, A., Suh, S., Du, S.W., Davis, J.R., Choi, E.H., Wang, X., Nielsen, S.C., Newby, G.A., Randolph, P.B., et al. (2022). Engineered virus-like particles for efficient in vivo delivery of therapeutic proteins. Cell *185*, 250–265.e16. https://doi.org/10.1016/j.cell.2021.12.021.

20. Lyu, P., Javidi-Parsijani, P., Atala, A., and Lu, B. (2019). Delivering Cas9/sgRNA ribonucleoprotein (RNP) by lentiviral capsid-based bionanoparticles for efficient 'hit-and-run' genome editing. Nucleic Acids Res. *47*, e99. https://doi.org/10.1093/nar/gkz605.

21. Haldrup, J., Andersen, S., Labial, A.R.L., Wolff, J.H., Frandsen, F.P., Skov, T.W., Rovsing, A.B., Nielsen, I., Jakobsen, T.S., Askou, A.L., et al. (2023). Engineered lentivirus-derived nanoparticles (LVNPs) for delivery of CRISPR/Cas ribonucleoprotein complexes supporting base editing, prime editing and in vivo gene modification. Nucleic Acids Res. *51*, 10059–10074. https://doi.org/10.1093/nar/gkad676.

22. Cronin, J., Zhang, X.-Y., and Reiser, J. (2005). Altering the Tropism of Lentiviral Vectors through Pseudotyping. Curr. Gene Ther. *5*, 387–398.

23. Gutierrez-Guerrero, A., Cosset, F.L., and Verhoeyen, E. (2020). Lentiviral Vector Pseudotypes: Precious Tools to Improve Gene Modification of Hematopoietic Cells for Research and Gene Therapy. Viruses *12*, 1016. https://doi.org/10.3390/v12091016.

24. Zhou, Q., Schneider, I.C., Edes, I., Honegger, A., Bach, P., Schönfeld, K., Schambach, A., Wels, W.S., Kneissl, S., Uckert, W., and Buchholz, C.J. (2012). T-cell receptor gene transfer exclusively to human CD8(+) cells enhances tumor cell killing. Blood *120*, 4334–4342. https://doi.org/10.1182/blood-2012-02-412973.

25. Bender, R.R., Muth, A., Schneider, I.C., Friedel, T., Hartmann, J., Plückthun, A., Maisner, A., and Buchholz, C.J. (2016). Receptor-Targeted Nipah Virus Glycoproteins Improve Cell-Type Selective Gene Delivery and Reveal a Preference for Membrane-Proximal Cell Attachment. PLoS Pathog. *12*, e1005641. https://doi.org/10.1371/journal.ppat.1005641.

26. Aiken, C. (1997). Pseudotyping Human Immunodeficiency Virus Type 1 (HIV-1) by the Glycoprotein of Vesicular Stromatitis Virus Targets HIV-1 Entry to an Endocytic Pathway and Suppresses both the Requirement for Nef and the Sensitivity of Cyclosporin A. J. Virol. *71*, 5871–5877.

27. Finkelshtein, D., Werman, A., Novick, D., Barak, S., and Rubinstein, M. (2013). LDL receptor and its family members serve as the cellular receptors for vesicular stomatitis virus. Proc. Natl. Acad. Sci. USA *110*, 7306–7311. https://doi.org/10.1073/pnas.1214441110.

28. Roche, S., Albertini, A.A.V., Lepault, J., Bressanelli, S., and Gaudin, Y. (2008). Structures of vesicular stomatitis virus glycoprotein: membrane fusion revisited. Cell. Mol. Life Sci. *65*, 1716–1728. https://doi.org/10.1007/s00018-008-7534-3.

29. Li, Q., Wu, J., Nie, J., Zhang, L., Hao, H., Liu, S., Zhao, C., Zhang, Q., Liu, H., Nie, L., et al. (2020). The Impact of Mutations in SARS-CoV-2 Spike on Viral Infectivity and Antigenicity. Cell *182*, 1284–1294.e9. https://doi.org/10.1016/j.cell.2020.07.012.

30. Harvey, W.T., Carabelli, A.M., Jackson, B., Gupta, R.K., Thomson, E.C., Harrison, E.M., Ludden, C., Reeve, R., Rambaut, A., et al.; COVID-19 Genomics UK COG-UK Consortium (2021). SARS-CoV-2 variants, spike mutations and immune escape. Nat. Rev. Microbiol. *19*, 409–424. https://doi.org/10.1038/s41579-021-00573-0.

31. Johnson, M.C., Lyddon, T.D., Suarez, R., Salcedo, B., LePique, M., Graham, M., Ricana, C., Robinson, C., and Ritter, D.G. (2020). Optimized Pseudotyping Conditions for the SARS-COV-2 Spike Glycoprotein. J. Virol. *94*, e01062-20. https://doi.org/10.1128/JVI.01062-20.

32. Crawford, K.H.D., Eguia, R., Dingens, A.S., Loes, A.N., Malone, K.D., Wolf, C.R., Chu, H.Y., Tortorici, M.A., Veesler, D., Murphy, M., et al. (2020). Protocol and Reagents for Pseudotyping Lentiviral Particles with SARS-CoV-2 Spike Protein for Neutralization Assays. Viruses *12*, 513. https://doi.org/10.3390/v12050513.

33. Schmidt, F., Weisblum, Y., Muecksch, F., Hoffmann, H.H., Michailidis, E., Lorenzi, J.C.C., Mendoza, P., Rutkowska, M., Bednarski, E., Gaebler, C., et al. (2020). Measuring SARS-CoV-2 neutralizing antibody activity using pseudotyped and chimeric viruses. J. Exp. Med. *217*, e20201181. https://doi.org/10.1084/jem.20201181.

34. Walls, A.C., Park, Y.J., Tortorici, M.A., Wall, A., McGuire, A.T., and Veesler, D. (2020). Structure, Function, and Antigenicity of the SARS-CoV-2 Spike Glycoprotein. Cell *181*, 281–292.e6. https://doi.org/10.1016/j.cell.2020.02.058.

35. Jackson, C.B., Farzan, M., Chen, B., and Choe, H. (2022). Mechanisms of SARS-CoV-2 entry into cells. Nat. Rev. Mol. Cell Biol. *23*, 3–20. https://doi.org/10.1038/s41580-021-00418-x.

36. Frecha, C., Costa, C., Negre, D., Gauthier, E., Russell, S.J., Cosset, F.L., and Verhoeyen, E. (2008). Stable transduction of quienscent T cells without induction of cycle progession by a novel lentiviral vector pseudotyped with measles virus glycoproteins. Blood *112*, 4843–4852. https://doi.org/10.1182/blood-2008-05-.

37. Frecha, C., Costa, C., Lévy, C., Nègre, D., Russell, S.J., Maisner, A., Salles, G., Peng, K.W., Cosset, F.L., and Verhoeyen, E. (2009). Efficient and stable transduction of resting B lymphocytes and primary chronic lymphocyte leukemia cells using measles virus gp displaying lentiviral vectors. Blood *114*, 3173–3180. https://doi.org/10.1182/blood-2009-05-220798.

38. Frecha, C., Lévy, C., Costa, C., Nègre, D., Amirache, F., Buckland, R., Russell, S.J., Cosset, F.L., and Verhoeyen, E. (2011). Measles virus glycoprotein-pseudotyped lentiviral vector-mediated gene transfer into quiescent lymphocytes requires binding to both SLAM and CD46 entry receptors. J. Virol. *85*, 5975–5985. https://doi.org/10.1128/JVI.00324-11.

39. Noyce, R.S., and Richardson, C.D. (2012). Nectin 4 is the epithelial cell receptor for measles virus. Trends Microbiol. *20*, 429–439. https://doi.org/10.1016/j.tim.2012.05.006.

40. Lin, L.T., and Richardson, C.D. (2016). The Host Cell Receptors for Measles Virus and Their Interaction with the Viral Hemagglutinin (H) Protein. Viruses *8*, 250. https://doi.org/10.3390/v8090250.

41. Funke, S., Schneider, I.C., Glaser, S., Mühlebach, M.D., Moritz, T., Cattaneo, R., Cichutek, K., and Buchholz, C.J. (2009). Pseudotyping lentiviral vectors with the wild-type measles virus glycoproteins improves titer and selectivity. Gene Ther. *16*, 700–705. https://doi.org/10.1038/gt.2009.11.

42. Manchester, M., Liszewski, M.K., Atkinson, J.P., and Oldstone, M.B. (1994). Multiple isoforms of CD46 (membrane cofactor protein) serve as Receptors for Measles Virus. Proc. Natl. Acad. Sci. USA *91*, 2161–2165.

43. Xu, K., Broder, C.C., and Nikolov, D.B. (2012). Ephrin-B2 and ephrin-B3 as functional henipavirus receptors. Semin. Cell Dev. Biol. *23*, 116–123. https://doi.org/10.1016/j.semcdb.2011.12.005.

44. Negrete, O.A., Levroney, E.L., Aguilar, H.C., Bertolotti-Ciarlet, A., Nazarian, R., Tajyar, S., and Lee, B. (2005). EphrinB2 is the entry receptor for Nipah virus, an emergent deadly paramyxovirus. Nature *436*, 401–405. https://doi.org/10.1038/nature03838.

45. Pernet, O., Pohl, C., Ainouze, M., Kweder, H., and Buckland, R. (2009). Nipah virus entry can occur by macropinocytosis. Virology *395*, 298–311. https://doi.org/10.1016/j.virol.2009.09.016.

46. Palomares, K., Vigant, F., Van Handel, B., Pernet, O., Chikere, K., Hong, P., Sherman, S.P., Patterson, M., An, D.S., Lowry, W.E., et al. (2013). Nipah virus envelope-pseudotyped lentiviruses efficiently target ephrinB2-positive stem cell populations in vitro and bypass the liver sink when administered in vivo. J. Virol. *87*, 2094–2108. https://doi.org/10.1128/JVI.02032-12.

47. Witting, S.R., Vallanda, P., and Gamble, A.L. (2013). Characterization of a third generation lentiviral vector pseudotyped with Nipah virus envelope proteins for endothelial cell transduction. Gene Ther. *20*, 997–1005. https://doi.org/10.1038/gt.2013.23.

48. Funke, S., Maisner, A., Mühlebach, M.D., Koehl, U., Grez, M., Cattaneo, R., Cichutek, K., and Buchholz, C.J. (2008). Targeted cell entry of lentiviral vectors. Mol. Ther. *16*, 1427–1436. https://doi.org/10.1038/mt.2008.128.

49. Slifka, M.K., Antia, R., Whitmire, J.K., and Ahmed, R. (1998). Humoral immunity due to long-lived plasma cells. Immunity *8*, 363–372.

50. Radbruch, A., Muehlinghaus, G., Luger, E.O., Inamine, A., Smith, K.G.C., Dörner, T., and Hiepe, F. (2006). Competence and competition: the challenge of becoming a long-lived plasma cell. Nat. Rev. Immunol. *6*, 741–750. https://doi.org/10.1038/nri1886.

51. Johnson, M.J., Laoharawee, K., Lahr, W.S., Webber, B.R., and Moriarity, B.S. (2018). Engineering of Primary Human B cells with CRISPR/Cas9 Targeted Nuclease. Sci. Rep. *8*, 12144. https://doi.org/10.1038/s41598-018-30358-0.

52. Hung, K.L., Meitlis, I., Hale, M., Chen, C.Y., Singh, S., Jackson, S.W., Miao, C.H., Khan, I.F., Rawlings, D.J., and James, R.G. (2018). Engineering Protein-Secreting Plasma Cells by Homology-Directed Repair in Primary Human B Cells. Mol. Ther. *26*, 456–467. https://doi.org/10.1016/j.ymthe.2017.11.012.

53. Laoharawee, K., Johnson, M.J., and Moriarity, B.S. (2020). CRISPR/Cas9-Mediated Genome Engineering of Primary Human B Cells. Methods Mol. Biol. *2115*, 435–444. https://doi.org/10.1007/978-1-0716-0290-4_24.

54. Moffett, H.F., Harms, C.K., Fitzpatrick, K.S., Tooley, M.R., Boonyaratanakornkit, J., and Taylor, J.J. (2019). B cells engineered to express pathogen-specific antibodies protect against infection. Sci. Immunol. *4*, eaax0644.

55. Nahmad, A.D., Raviv, Y., Horovitz-Fried, M., Sofer, I., Akriv, T., Nataf, D., Dotan, I., Carmi, Y., Burstein, D., Wine, Y., et al. (2020). Engineered B cells expressing an anti-HIV antibody enable memory retention, isotype switching and clonal expansion. Nat. Commun. *11*, 5851. https://doi.org/10.1038/s41467-020-19649-1.

56. Nahmad, A.D., Lazzarotto, C.R., Zelikson, N., Kustin, T., Tenuta, M., Huang, D., Reuveni, I., Nataf, D., Raviv, Y., Horovitz-Fried, M., et al. (2022). In vivo engineered B cells secrete high titers of broadly neutralizing anti-HIV antibodies in mice. Nat. Biotechnol. *40*, 1241–1249. https://doi.org/10.1038/s41587-022-01328-9.

57. Giroglou, T., Cinatl, J., Jr., Rabenau, H., Drosten, C., Schwalbe, H., Doerr, H.W., and von Laer, D. (2004). Retroviral vectors pseudotyped with severe acute respiratory syndrome coronavirus S protein. J. Virol. *78*, 9007–9015. https://doi.org/10.1128/JVI.78.17.9007-9015.2004.

58. Liu, Y., Liu, J., Plante, K.S., Plante, J.A., Xie, X., Zhang, X., Ku, Z., An, Z., Scharton, D., Schindewolf, C., et al. (2022). The N501Y spike substitution enhances SARS-CoV-2 infection and transmission. Nature *602*, 294–299. https://doi.org/10.1038/s41586-021-04245-0.

59. Ozog, S., Chen, C.X., Simpson, E., Garijo, O., Timberlake, N.D., Minder, P., Verhoeyen, E., and Torbett, B.E. (2019). CD46 Null Packaging Cell Line Improves Measles Lentiviral Vector Production and Gene Delivery to Hematopoietic Stem and Progenitor Cells. Mol. Ther. Methods Clin. Dev. *13*, 27–39. https://doi.org/10.1016/j.omtm.2018.11.006.

60. Humbert, J.M., Frecha, C., Amirache Bouafia, F., N'Guyen, T.H., Boni, S., Cosset, F.L., Verhoeyen, E., and Halary, F. (2012). Measles virus glycoprotein-pseudotyped lentiviral vectors are highly superior to vesicular stomatitis virus G pseudotypes for genetic modification of monocyte-derived dendritic cells. J. Virol. *86*, 5192–5203. https://doi.org/10.1128/JVI.06283-11.

61. Girard-Gagnepain, A., Amirache, F., Costa, C., Lévy, C., Frecha, C., Fusil, F., Nègre, D., Lavillette, D., Cosset, F.L., and Verhoeyen, E. (2014). Baboon envelope pseudotyped LVs outperform VSV-G-LVs for gene transfer into early-cytokine-stimulated and resting HSCs. Blood *124*, 1221–1231. https://doi.org/10.1182/blood-2014-02-.

62. Mangeot, P.E., Risson, V., Fusil, F., Marnef, A., Laurent, E., Blin, J., Mournetas, V., Massouridès, E., Sohier, T.J.M., Corbin, A., et al. (2019). Genome editing in primary cells and in vivo using viral-derived Nanoblades loaded with Cas9-sgRNA ribonucleoproteins. Nat. Commun. *10*, 45. https://doi.org/10.1038/s41467-018-07845-z.

63. Hamilton, J.R., Chen, E., Perez, B.S., Sandoval Espinoza, C.R., Kang, M.H., Trinidad, M., Ngo, W., and Doudna, J.A. (2024). In vivo human T cell engineering with enveloped delivery vehicles. Nat. Biotechnol. https://doi.org/10.1038/s41587-023-02085-z.

64. Maule, G., Arosio, D., and Cereseto, A. (2020). Gene Therapy for Cystic Fibrosis: Progress and Challenges of Genome Editing. Int. J. Mol. Sci. *21*, 3903. https://doi.org/10.3390/ijms21113903.

65. Nakamura, T., Peng, K.W., Harvey, M., Greiner, S., Lorimer, I.A.J., James, C.D., and Russell, S.J. (2005). Rescue and propagation of fully retargeted oncolytic measles viruses. Nat. Biotechnol. *23*, 209–214. https://doi.org/10.1038/nbt1060.

66. Anliker, B., Abel, T., Kneissl, S., Hlavaty, J., Caputi, A., Brynza, J., Schneider, I.C., Münch, R.C., Petznek, H., Kontermann, R.E., et al. (2010). Specific gene transfer to neurons, endothelial cells and hematopoietic progenitors with lentiviral vectors. Nat. Methods *7*, 929–935. https://doi.org/10.1038/nmeth.1514.

67. Vamva, E., Ozog, S., Verhoeyen, E., James, R.G., Rawlings, D.J., and Torbett, B.E. (2022). An optimized measles virus glycoprotein-pseudotyped lentiviral vector production system to promote efficient transduction of human primary B cells. STAR Protoc. *3*, 101228. https://doi.org/10.1016/j.xpro.2022.101228.

68. Levy, C., Amirache, F., Costa, C., Frecha, C., Muller, C.P., Kweder, H., Buckland, R., Cosset, F.L., and Verhoeyen, E. (2012). Lentiviral vectors displaying modified measles virus gp overcome pre-existing immunity in in vivo-like transduction of human T and B cells. Mol. Ther. *20*, 1699–1712. https://doi.org/10.1038/mt.2012.96.

69. Kneissl, S., Abel, T., Rasbach, A., Brynza, J., Schneider-Schaulies, J., and Buchholz, C.J. (2012). Measles virus glycoprotein-based lentiviral targeting vectors that avoid neutralizing antibodies. PLoS One *7*, e46667. https://doi.org/10.1371/journal.pone.0046667.

70. Rogers, G.L., and Cannon, P.M. (2021). Genome edited B cells: a new frontier in immune cell therapies. Mol. Ther. *29*, 3192–3204. https://doi.org/10.1016/j.ymthe.2021.09.019.

71. Luo, B., Zhan, Y., Luo, M., Dong, H., Liu, J., Lin, Y., Zhang, J., Wang, G., Verhoeyen, E., Zhang, Y., and Zhang, H. (2020). Engineering of alpha-PD-1 antibody-expressing long-lived plasma cells by CRISPR/Cas9-mediated targeted gene integration. Cell Death Dis. *11*, 973. https://doi.org/10.1038/s41419-020-03187-1.

72. Zhou, Q., Schneider, I.C., Gallet, M., Kneissl, S., and Buchholz, C.J. (2011). Resting lymphocyte transduction with measles virus glycoprotein pseudotyped lentiviral vectors relies on CD46 and SLAM. Virology *413*, 149–152. https://doi.org/10.1016/j.virol.2011.02.010.

73. Takano, K.A., Wong, A.A.L., Brown, R., Situ, K., Chua, B.A., Abu, A.E., Pham, T.T., Reyes, G.C., Ramachandran, S., Kamata, M., et al. (2024). Envelope protein-specific B cell receptors direct lentiviral vector tropism in vivo. Mol. Ther. *32*, 1311–1327. https://doi.org/10.1016/j.ymthe.2024.03.002.

74. An, M., Raguram, A., Du, S.W., Banskota, S., Davis, J.R., Newby, G.A., Chen, P.Z., Palczewski, K., and Liu, D.R. (2024). Engineered virus-like particles for transient delivery of prime editor ribonucleoprotein complexes in vivo. Nat. Biotechnol. https://doi.org/10.1038/s41587-023-02078-y.

75. Brinkman, E.K., Chen, T., Amendola, M., and van Steensel, B. (2014). Easy quantitative assessment of genome editing by sequence trace decomposition. Nucleic Acids Res. *42*, e168. https://doi.org/10.1093/nar/gku936.

76. Hsiau, T., Conant, D., Maures, T., Waite, K., Yang, J., Kelso, R., Holden, K., Enzmann, B.L., and Stoner, R. (2022). Inference of CRISPR Edits from Sanger Trace Data. CRISPR J. *5*, 123–130. https://doi.org/10.1101/251082.